RESEARCH ARTICLE

The kinase PDK1 is critical for promoting T follicular helper cell differentiation

Zhen Sun[1†], Yingpeng Yao[1†], Menghao You[1†], Jingjing Liu[1], Wenhui Guo[1], Zhihong Qi[1], Zhao Wang[1], Fang Wang[1], Weiping Yuan[2], Shuyang Yu[1]*

[1]State Key Laboratory of Agrobiotechnology, College of Biological Sciences, China Agricultural University, Beijing, China; [2]State Key Laboratory of Experimental Hematology, Institute of Hematology and Blood Diseases Hospital, and Center for Stem Cell Medicine, Chinese Academy of Medical Sciences and Peking Union Medical College, Tianjin, China

Abstract The kinase PDK1 is a crucial regulator for immune cell development by connecting PI3K to downstream AKT signaling. However, the roles of PDK1 in $CD4^+$ T cell differentiation, especially in T follicular helper (Tfh) cell, remain obscure. Here we reported PDK1 intrinsically promotes the Tfh cell differentiation and germinal center responses upon acute infection by using conditional knockout mice. PDK1 deficiency in T cells caused severe defects in both early differentiation and late maintenance of Tfh cells. The expression of key Tfh regulators was remarkably downregulated in PDK1-deficient Tfh cells, including *Tcf7*, *Bcl6*, *Icos*, and *Cxcr5*. Mechanistically, ablation of PDK1 led to impaired phosphorylation of AKT and defective activation of mTORC1, resulting in substantially reduced expression of Hif1α and p-STAT3. Meanwhile, decreased p-AKT also suppresses mTORC2-associated GSK3β activity in PDK1-deficient Tfh cells. These integrated effects contributed to the dramatical reduced expression of TCF1 and ultimately impaired the Tfh cell differentiation.

***For correspondence:** ysy@cau.edu.cn

[†]These authors contributed equally to this work

Competing interests: The authors declare that no competing interests exist.

Funding: See page 17

Received: 24 July 2020
Accepted: 08 February 2021
Published: 17 February 2021

Reviewing editor: Bernard Malissen, Centre d'Immunologie de Marseille-Luminy, Aix Marseille Université, France

Introduction

The serine/threonine kinase 3-phosphoinositide-dependent protein kinase 1 (PDK1) is a critical metabolic regulator connecting PI3K and downstream molecules (***Park et al., 2009***). PDK1 is crucial for multiple types of immune cell development, such as hematopoietic stem cells, B cells, NK cells, T cells, and cytolytic $CD8^+$ cells (***Park et al., 2009***; ***Baracho et al., 2014***; ***Venigalla et al., 2013***; ***Yang et al., 2015***; ***Finlay et al., 2012***). Despite these profound effects of PDK1 on the regulation of various immune cell subsets, its role in $CD4^+$ T helper cells, especially T follicular helper (Tfh) cell differentiation, has not been experimentally determined.

Upon foreign antigens challenge, naïve $CD4^+$ T cells differentiate into functionally distinct subsets. Tfh cells are a specialized population that provides cognate help in germinal center (GC) to facilitate immunoglobulin affinity maturation and heavy-chain class switching, and ultimately promote generation of high-affinity antibodies of diverse isotypes, long-lived plasma cells, and memory B cells (***Crotty, 2014***). The characteristic features of Tfh cells are defined as expression of the CXCR5, ICOS, PD-1, Bcl-6, and IL-21 (***Crotty, 2019***). Differentiation of Tfh cell relies on precisely orchestrated transcriptional program, which lies in the mutually antagonistic Bcl-6-Blimp1 as the core regulatory axis. Bcl-6 is indispensable for the divergence of $CD4^+$ T cells into Tfh lineage, whereas Blimp1 programs Th1 cell formation (***Johnston et al., 2009***; ***Yu et al., 2009***; ***Nurieva et al., 2009***). TCF1 (encoded by *Tcf7*) supports Tfh cell specification by promoting Bcl-6 and repressing Blimp1 expression, revealing a key role of TCF1 in the regulation of the Bcl-6-Blimp1 axis (***Shao et al., 2019***; ***Wu et al., 2015***; ***Choi et al., 2015***; ***Xu et al., 2015***).

Compared with other T helper cells, the differentiation of Tfh is more dependent on signals provided by both TCR and co-receptors (**Deenick et al., 2010**; **Baumjohann et al., 2013**). Except sustained TCR signals, Tfh cells also express high levels of many co-receptors for their generation and function, including CD28 and ICOS (**Qin et al., 2018**). The PI3K signaling via AKT is responsible for transduction of Tfh cell-dependent TCR signals and ICOS co-stimulation and essential for Tfh cell differentiation. Previous studies have revealed inactivation of PI3K catalytic subunit p110δ or regulatory subunit p85α almost completely abolishes Tfh cell differentiation (**Rolf et al., 2010**; **Leavenworth et al., 2015**), whereas mice that express the E1020K activating mutant of p110δ or have a T cell-specific deficiency of PTEN exhibit enhanced Tfh cell formation (**Preite et al., 2018a**; **Shrestha et al., 2015**). Moreover, FoxO1, which is suppressed by AKT, restrains Tfh cell differentiation (**Stone et al., 2015**). Besides, PI3K-mediated signaling pathways involving mTORC1 and mTORC2 are also critical for Tfh cells. mTORC1 induces p-S6 and Glut1 expression to promote protein synthesis and cell proliferation, essential events for Tfh cell specification (**Zeng et al., 2016**). Unlike mTORC1, mTORC2 programs Tfh cell differentiation by decreasing FoxO1 activity and transcriptionally regulates signature programming of Tfh cells, including *Bcl6*, *Cxcr5*, and *Tcf7* (**Hao et al., 2018**). Correspondingly, Yang et al. reported mTORC2-deficient $CD4^+$ T cells show reduced p-GSK3β, β-catenin, and TCF1 level, establishing a positive link between PI3K/AKT and Wnt/β-catenin/TCF1 signaling (**Yang et al., 2016**). Besides, mTOR-dependent Hif activity is also crucial for Tfh cell development (**Cho et al., 2019**).

In this study, we explore the knowledge gap whether and how PDK1 plays essential roles in Tfh cell differentiation elicited by acute viral infection and protein immunization. Our data indicated that PDK1 is intrinsically required for Tfh cell formation and effector functions, which is important to understanding the nature of the Tfh cell development.

Results

PDK1 promotes Tfh cell differentiation and GC Bcell responses

To elucidate whether PDK1 regulates Tfh cell differentiation, we first evaluated the expression of PDK1 in bifurcation of effector $CD4^+$ T cells into Tfh or Th1 cells upon acute viral infection (**Xu et al., 2015**). We infected wild-type C57BL/6J mice with LCMV Armstrong strain and observed elevated expression level of PDK1 in Tfh cells compared with naïve $CD4^+$ T or Th1 cells on day 8 post-infection (8 dpi), which suggested potential roles of PDK1 in Tfh cells (**Figure 1A**). To further investigate the function of PDK1 in Tfh cells, we generated conditionally knockout mice ($Pdk1^{fl/fl}$::*Cd4*-Cre mice), and the deletion efficiency in $CD4^+$ T cells was further confirmed by quantitative RT-PCR (**Figure 1B**). Next, $Pdk1^{fl/fl}$::*Cd4*-Cre mice and their wild-type littermates (WT) were infected with LCMV Armstrong. On 8 dpi, generations of Tfh cells (26.5-fold) and Th1 cells (2.6-fold) were substantially decreased in $Pdk1^{fl/fl}$::*Cd4*-Cre mice (**Figure 1C,D**), indicating PDK1 has a more crucial role for Tfh cell differentiation. Moreover, GC Tfh cells were also significantly reduced in PDK1-deficient mice (**Figure 1C,D**). Consistently, the expression levels of PD-1, ICOS, and Bcl-6 were much lower in $Pdk1^{fl/fl}$::*Cd4*-Cre Tfh cells than those of WT cells (**Figure 1E,F**). Collectively, these data indicated that PDK1 is essential for Tfh cell differentiation during viral infection.

High expression of CXCR5, which is the B-cell homing chemokine CXCL13-responding receptor, allows Tfh cells to access the B-cell follicle (**Crotty, 2011**), Tfh cells then support GC formation and effective humoral immunity (**Crotty, 2019**). Thus, we first analyzed Tfh cell migratory response toward CXCL13. $Pdk1^{fl/fl}$::*Cd4*-Cre Tfh cells exhibited severe defects in migratory response toward CXCL13 (**Figure 1G**), indicating impairment of the follicular migratory potential of Tfh cells in the absence of PDK1 may constrain GC responses. We next examined the effects on GC B-cell responses due to PDK1 deficiency. Flow cytometry analysis revealed GC B cells and plasma cells were profoundly impaired in $Pdk1^{fl/fl}$::*Cd4*-Cre mice compared with WT mice (**Figure 1H,I**). In concert with decreased GC B cells, PNA^+ GCs areas in spleens of $Pdk1^{fl/fl}$::*Cd4*-Cre mice were also smaller than those in WT littermates (**Figure 1J**). Correspondingly, the concentrations of LCMV-specific IgG in the serum of $Pdk1^{fl/fl}$::*Cd4*-Cre mice were much lower than WT mice on 8 dpi and 56 dpi (**Figure 1K**). These data corroborated an indispensable role of PDK1 in Tfh and GC B-cell differentiation as well as antibody production.

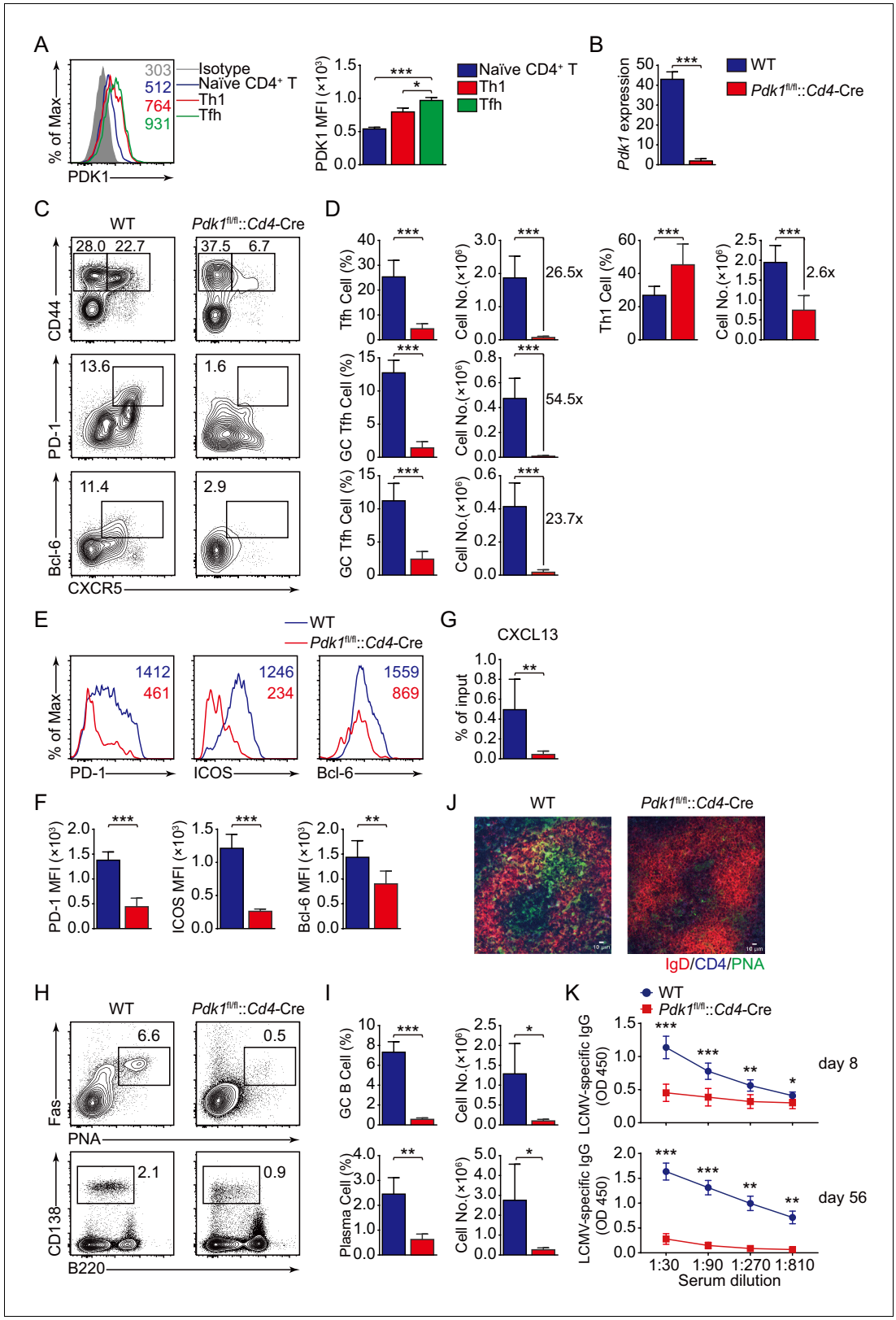

Figure 1. PDK1 supports Tfh cell differentiation and effector functions. (**A**) Flow cytometry analysis of PDK1 expression in naïve CD4$^+$ T (CD62L^{hi}CD44^{lo}), Th1, and Tfh cells from C57BL/6J mice on 8 dpi. Quantification of PDK1 MFI is shown on the right (n = 8). (**B**) Quantitative RT-PCR analysis of *Pdk1* abundance in naïve CD4$^+$ T cells, from WT and *Pdk1*$^{fl/fl}$::*Cd4*-Cre mice (*n* = 3). (**C, D**) Flow cytometry analysis of CD44$^+$CXCR5$^+$ Tfh cells and CD44$^+$CXCR5$^-$ Th1 cells gated on total CD4$^+$ T cells (top panel), or PD-1^{hi}CXCR5$^+$ GC Tfh cells (middle panel) and Bcl-6^{hi}CXCR5$^+$ GC Tfh cells

Figure 1 continued on next page

Figure 1 continued

(bottom panel) gated on $CD44^+CD62L^-CD4^+$ T cells from spleens of WT and *Pdk1*$^{fl/fl}$::*Cd4*-Cre mice on 8 dpi with representative contour plots and cumulative data in (**C**) and (**D**), respectively (n ≥ 6). (**E, F**) Expression of PD-1, ICOS, and Bcl-6 on Tfh cells ($CD4^+CD44^+CXCR5^+$) was analyzed by flow cytometry with representative histograms and quantification data in (**E**) and (**F**), respectively (n = 6). (**G**) Chemotaxis transwell assay for Tfh cells. Splenocytes from WT and *Pdk1*$^{fl/fl}$::*Cd4*-Cre mice on 8 dpi were added to a transwell plate and migration in the presence of CXCL13 was assessed (n ≥ 5). (**H, I**) Flow cytometry analysis of splenic PNA^+Fas^+ GC B cells (top panel) and $B220^-CD138^+$ plasma cells (bottom panel) from WT and *Pdk1*$^{fl/fl}$::*Cd4*-Cre mice on 8 dpi with representative contour plots and cumulative data in (**H**) and (**I**), respectively (n = 4). (**J**) Confocal microscopy analysis of GC histology in spleen sections from WT and *Pdk1*$^{fl/fl}$::*Cd4*-Cre mice on 8 dpi. Green: PNA, red: IgD, blue: CD4; scale bar: 10 μm. (**K**) LCMV-specific IgG concentration of sera from WT and *Pdk1*$^{fl/fl}$::*Cd4*-Cre mice on day 8 (top panel) and 56 (bottom panel) post-infection was measured by ELISA (n ≥ 7). Data are representative of at least two independent experiments (**A, B, E–G, H–I, K**) or pooled from three independent experiments (**C, D**). Error bars represent SD. *p<0.05, **p<0.01, and ***p<0.001 (Student's t-test).

The online version of this article includes the following source data for figure 1:

Source data 1. PDK1 supports Tfh cell differentiation and effector functions.

To validate the findings by using LCMV Armstrong infection approach, we also analyzed Tfh cell response upon KLH immunization. Consistent with the results shown above, loss of PDK1 led to significant reduction of Tfh cells as well as impaired expression of Tfh markers on day 8 post-KLH immunization (***Figure 2A–D***). Besides, both GC B cells and plasma cells were decreased in *Pdk1*$^{fl/fl}$::*Cd4*-Cre mice (***Figure 2E,F***). These data collectively demonstrated that PDK1 positively regulates Tfh cell differentiation and effector functions upon different antigens challenge.

In addition, we also analyzed the production of signature cytokines for other $CD4^+$ T cell subsets, such as IFNγ, IL-4, or IL-17a, in KLH-immunized WT and *Pdk1*$^{fl/fl}$::*Cd4*-Cre mice. $CD4^+$ T cells from *Pdk1*$^{fl/fl}$::*Cd4*-Cre mice showed greater expression of IFNγ, IL-4, and IL-17a than those in WT mice (***Figure 2—figure supplement 1***), which is consistent with previous report (***Yu et al., 2015***). These results indicated that PDK1 may also involve in other T helper cell differentiation under immunized condition.

Intrinsic impact of PDK1 on Tfh cell development

To precisely clarify the cell-intrinsic role of PDK1 in regulating Tfh cell responses, we generated bone marrow (BM) chimeras by reconstituting lethally irradiated recipients ($CD45.1^+$ $CD45.2^+$) with a mixture of donor BM cells from *Pdk1*$^{fl/fl}$::*Cd4*-Cre or WT mice ($CD45.2^+$) with $CD45.1^+CD45.2^+$ WT mice (***Figure 3A***). After successful reconstitution (***Figure 3B***), we infected the chimeric mice with LCMV Armstrong and analyzed Tfh cells on 8 dpi. We first gated $CD44^+CXCR5^+$ Tfh cells, PD-$1^{hi}CXCR5^+$ GC Tfh cells, and Bcl-$6^{hi}CXCR5^+$ GC Tfh cells, and then the contributions of $CD45.2^+$ cells from WT or *Pdk1*$^{fl/fl}$::*Cd4*-Cre mice were analyzed. We found $CD45.2^+$ cells from *Pdk1*$^{fl/fl}$::*Cd4*-Cre mice only accounted for less than 1% of the total Tfh cells and GC Tfh cells, while $CD45.2^+$ cells of WT origin contributed to 23.1–29.7% among Tfh and GC Tfh cells (***Figure 3C–E***). Additionally, the expression levels of PD-1, ICOS, and Bcl-6 were substantially reduced in *Pdk1*$^{fl/fl}$::*Cd4*-Cre Tfh cells compared with WT cells (***Figure 3F,G***). Collectively, these data thus confirmed the intrinsic role of PDK1 in regulating Tfh cell differentiation.

PDK1 is required for Tfh cells at both early and late stages

To investigate the role of PDK1 in early commitment or late maturation of Tfh cell differentiation, we bred *Pdk1*$^{fl/fl}$::*Rosa26*^{CreER} mice with SMARTA mice to generate *Pdk1*$^{fl/fl}$::*Rosa26*^{CreER}::SMARTA mice, which enabled us to carry out the adoptive transfer assay by induced ablation of PDK1 with Tamoxifen at early stage of Tfh cell differentiation. We transferred WT or *Pdk1*$^{fl/fl}$::*Rosa26*^{CreER}::SMARTA cells into congenic recipient mice, which were then administrated with Tamoxifen followed by LCMV Armstrong infection (***Figure 4A,B***). On 3 dpi, both the frequency and cell numbers of Bcl-6^+CXCR5^+ Tfh cells of *Pdk1*$^{fl/fl}$::*Rosa26*^{CreER}::SMARTA mice were remarkably decreased compared with those of WT counterparts (***Figure 4C***). Moreover, both PDK1-deficient activated $CD4^+$ T cells and $CXCR5^+$ Tfh cells exhibited slower proliferation (***Figure 4D***), while the apoptosis was not altered in these cells (***Figure 4—figure supplement 1A***). We further sorted $CXCR5^+$ Tfh cells and performed quantitative RT-PCR analysis. The expression of Tfh cell-related genes *Tcf7*, *Cxcr5*, *Bcl6*, and *Pdcd1* was remarkably decreased in PDK1-deficient Tfh cells (***Figure 4E***). These results suggested that PDK1 is essential for proliferation and commitment of early Tfh cells.

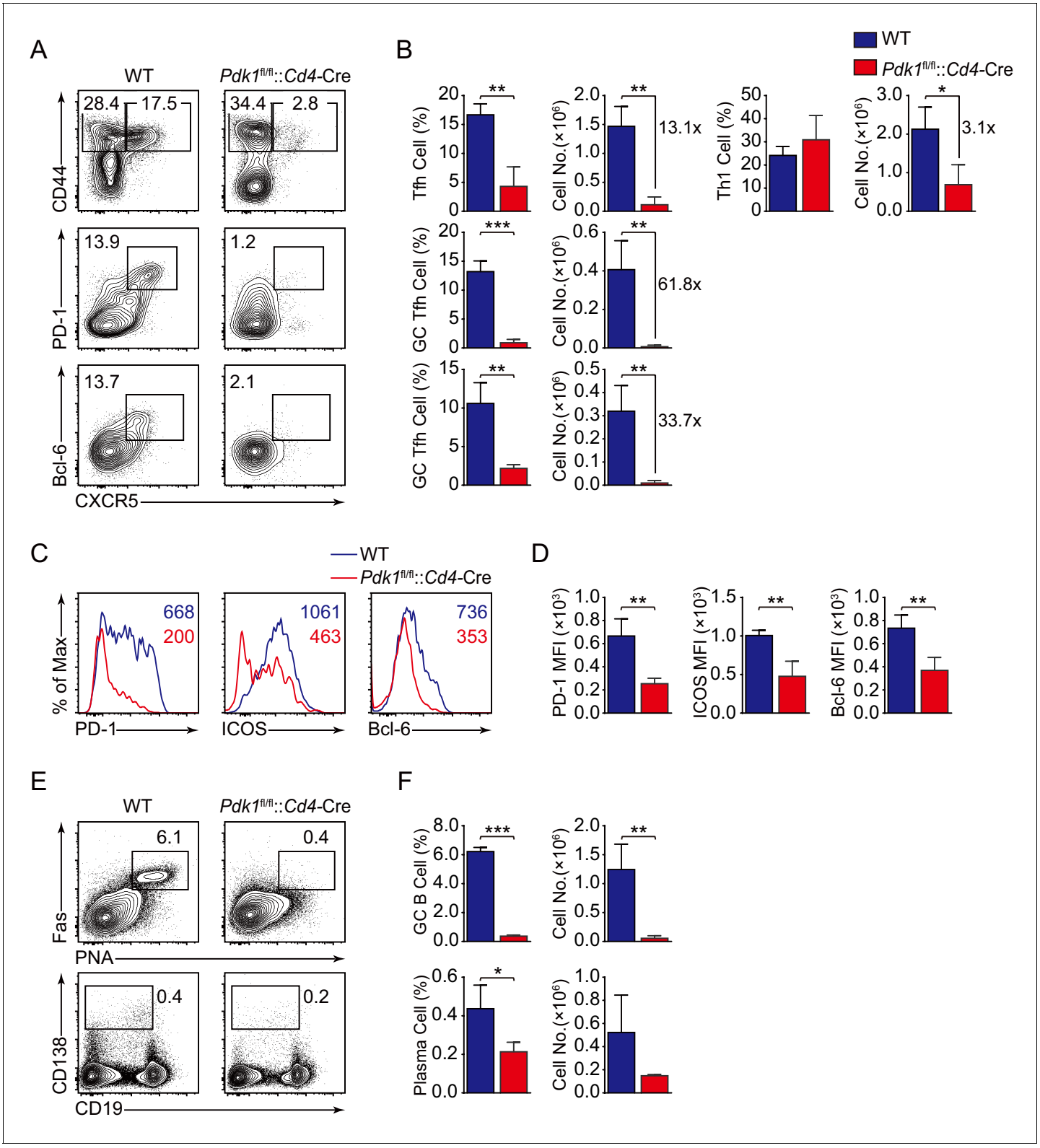

Figure 2. PDK1 is essential for Tfh cell differentiation upon protein immunization. (**A, B**) Flow cytometry analysis of $CD44^+CXCR5^+$ Tfh cells and $CD44^+CXCR5^-$ Th1 cells gated on splenic $CD4^+$ T cells (top panel) or PD-$1^{hi}CXCR5^+$ GC Tfh cells (middle panel) and Bcl-$6^{hi}CXCR5^+$ GC Tfh cells (bottom panel) gated on splenic $CD44^+CD62L^-CD4^+$ T cells from WT and *Pdk1*$^{fl/fl}$::*Cd4*-Cre mice on day 8 post-KLH immunization with representative contour plots and cumulative data in (**A**) and (**B**), respectively (n = 3). (**C, D**) Expression of PD-1, ICOS, and Bcl-6 on Tfh cells ($CD4^+CD44^+CXCR5^+$) was analyzed by flow cytometry with representative histograms and quantification data in (**C**) and (**D**), respectively (n = 3). (**E, F**) Flow cytometry analysis of

Figure 2 continued on next page

Figure 2 continued

splenic PNA$^+$Fas$^+$ GC B cells (top panel) and B220$^-$CD138$^+$ plasma cells (bottom panel) from WT and *Pdk1*$^{fl/fl}$::*Cd4*-Cre mice on day 8 post-KLH immunization with representative contour plots and cumulative data in (**E**) and (**F**), respectively (n = 3). Data are representative of two independent experiments. Error bars represent SD. *p<0.05, **p<0.01, and ***p<0.001 (Student's t-test).

The online version of this article includes the following source data and figure supplement(s) for figure 2:

Source data 1. PDK1 is essential for Tfh cell differentiation and GC responses upon KLH immunization.
Figure supplement 1. Analysis of T helper cells upon KLH immunization.
Figure supplement 1—source data 1. Analysis of distinct T helper subsets upon KLH immunization.

To specifically delete PDK1 at the late stage of Tfh cell differentiation, we treated WT or *Pdk1*$^{fl/fl}$::*Rosa26*^{CreER} mice with tamoxifen from day 4 to day 7 post-viral infection (***Figure 4F,G***). On 8 dpi, we observed decreased Tfh cells and GC Tfh cells in tamoxifen-treated *Pdk1*$^{fl/fl}$::*Rosa26*^{CreER} mice (***Figure 4H***). Moreover, both activated CD4$^+$ T cells and CXCR5$^+$CD44$^+$ Tfh cells showed slower proliferation in the absence of PDK1 (***Figure 4I***). While the apoptosis of these two subsets was not affected (***Figure 4—figure supplement 1B***). These results indicated that PDK1 is also required for expansion and maintenance of late Tfh cell.

PDK1-dependent Tfh cell transcriptomes

To further elucidate the mechanisms, we next explored how PDK1 deficiency impacts Tfh cell transcriptomes. CD44$^+$SLAM^{lo} Tfh cells were sorted from LCMV Armstrong-infected *Pdk1*$^{fl/fl}$::*Cd4*-Cre and WT mice on 8 dpi and subjected to RNA-seq. One thousand two hundred and thirty-eight upregulated and 354 downregulated genes in PDK1-deficient Tfh cells were identified by RNA-seq analysis (***Figure 5A***). Moreover, a dysregulation of diverse pathways was observed, in particular PI3K-AKT signaling pathway (***Figure 5B***). Then, we selected a Tfh gene set (***Choi et al., 2015***) for gene set enrichment analysis (GSEA). The Tfh signature genes were negatively enriched in *Pdk1*$^{fl/fl}$::*Cd4*-Cre Tfh cells (***Figure 5C***). We further selected some interested differentially expressed genes (DEGs) from the RNA-seq results and confirmed their alterations by quantitative RT-PCR. We found the expression of Tfh cell-related genes *Cxcr5*, *Bcl6*, *Tcf7*, and *Icos* was decreased in PDK1-deficient Tfh cells compared with those of WT cells (***Figure 5D***). The expression of *Maf*, which encodes transcription factor c-Maf, inducing IL-21 expression in Tfh cells to support GC response (***Bauquet et al., 2009***), was decreased in PDK1-deficient Tfh cells compared with WT cells (***Figure 5D***). Moreover, the expression of *Hif1a*, which supports Tfh cell formation (***Cho et al., 2019***; ***He et al., 2019***), was substantially lower in PDK1-null Tfh cells (***Figure 5D***). Whereas expression of other effector cells-relevant genes *Gzmb* (which encodes granzyme B), *Id2*, *Gata3*, and *Prdm1* was higher in PDK1-null Tfh cells than those in WT cells (***Figure 5D***). Taken together, these data strongly suggested that PDK1 is indispensable for maintaining Tfh cell identity.

Given Tfh cell differentiation is largely dependent on TCR and co-receptor pathways (***Fazilleau et al., 2009***; ***Tubo et al., 2013***), we next questioned which signaling acts on upstream of PDK1 in Tfh cells. To achieve this goal, we performed GSEA with gene sets related to CD28- and ICOS-dependent pathways. *Pdk1*$^{fl/fl}$::*Cd4*-Cre Tfh cells showed reduced expression of signatures in the gene set 'Up-regulated under anti-CD28' containing up-regulated genes upon anti-CD28 stimulation (***Figure 5E***). Moreover, *Pdk1*$^{fl/fl}$::*Cd4*-Cre Tfh cells showed increased expression of signatures in the gene set 'Down-regulated under anti-ICOS-L' containing down-regulated genes upon ICOS-L blocking (***Figure 5E***). These analyses suggested that CD28- or ICOS-dependent PDK1 activity may involve in Tfh cell differentiation. To further validate this, we stimulated CD4$^+$ T cells isolated from GP61-primed WT SMARTA mice with different stimuli combinations, including anti-CD3e plus anti-CD28, anti-CD3e plus anti-ICOS, anti-CD3e plus anti-CD28 plus anti-CD28, anti-ICOS only, or CD25 only (***Figure 5F,G***). We then measured the level of AKT phosphorylation at T308, which is an indicator of PDK1 activity. The results indicated that anti-ICOS only could elicit higher level of p-AKT^{T308}, and combination of anti-ICOS plus anti-CD3e or/and anti-CD28 had a similar effect with anti-ICOS only (***Figure 5F,G***). These results further strengthen the notion that ICOS-dependent PDK1 activity is essential for Tfh cells, which is corresponding to the previous report that ICOS-driven PI3K signaling is indispensable for Tfh cell differentiation (***Gigoux et al., 2009***).

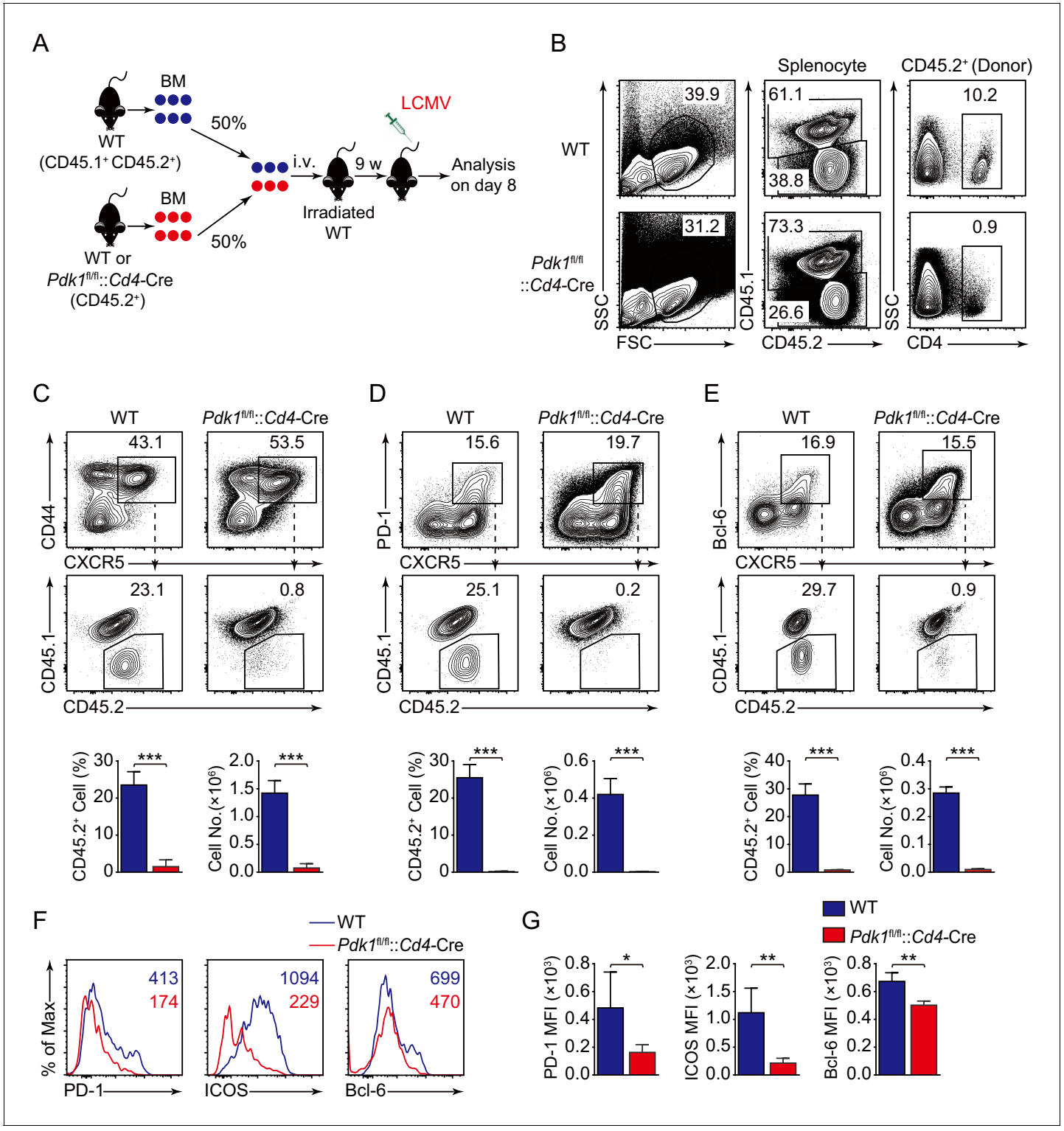

Figure 3. PDK1 intrinsically regulates Tfh cell differentiation. (**A**) Generation of bone marrow (BM) chimeric mice. BM cells from WT or *Pdk1*$^{fl/fl}$::*Cd4*-Cre mice (CD45.2$^+$) were mixed with WT (CD45.1$^+$CD45.2$^+$) competitor cells at a 1:1 ratio, and transferred to lethally irradiated WT recipients (CD45.1$^+$CD45.2$^+$). After 9 weeks reconstitution, the recipients were infected with LCMV and analyzed 8 days later. (**B**) Analysis of chimerism by flow cytometry. WT and *Pdk1*$^{fl/fl}$::*Cd4*-Cre cells (CD45.2$^+$) in CD4$^+$ T cells of chimera mice were determined. (**C–E**) Flow cytometry analysis of competitive contributions by CD45.2$^+$ cells to the total CD44$^+$CXCR5$^+$ Tfh (**C**), PD-1^{hi}CXCR5$^+$ GC Tfh (**D**), and Bcl-6^{hi}CXCR5$^+$ Tfh (**E**) cell population from recipients with representative contour plots and cumulative data (n = 4). (**F, G**) Detection of PD-1, ICOS, and Bcl-6 expression on CD44$^+$CXCR5$^+$ Tfh cells from

Figure 3 continued on next page

Figure 3 continued

recipients by flow cytometry with representative histograms and quantification data in (**F**) and (**G**), respectively (n = 4). Data are representative of two independent experiments. Error bars represent SD. *p<0.05, **p<0.01, and ***p<0.001 (Student's t-test).
The online version of this article includes the following source data for figure 3:

Source data 1. PDK1 intrinsically programs Tfh cell differentiation.

PDK1 modulates TCF1 expression to program Tfh cell differentiation corresponding to both mTORC1 and mTORC2 signals

We next explored the potential targets of PDK1 involving in regulation on Tfh cells. We first looked at the effects of PDK1 deficiency on its downstream signaling by GSEA. We observed both Raptor and Rictor-activated genes were significantly enriched in WT Tfh cells, while Raptor and Rictor-suppressed genes were remarkably enriched in *Pdk1*$^{fl/fl}$::*Cd4*-Cre Tfh cells. These results indicated that PDK1 and mTORC1/mTORC2 regulate a common subset of target genes in the Tfh cells (***Figure 6A***). We then determined these downstream signaling by flow cytometry analysis. We found *Pdk1*$^{fl/fl}$::*Cd4*-Cre Tfh cells showed decreased amounts of both basal and phosphorylation of AKT at T308 and S473 compared with WT cells (***Figure 6B***), which were consistent with previous observations in B cells (***Venigalla et al., 2013***), suggesting phosphorylation of AKT at T308 and S473 was interdependent in Tfh cells. However, the phosphorylation level of PKCζ/λ, another target of PDK1, was comparable between PDK1-deficient and WT Tfh cells (***Figure 6—figure supplement 1A***). AKT phosphorylates FoxOs, and we observed both basal and phosphorylation levels of FoxO1/3a were substantially reduced in PDK1-deficient Tfh cells (***Figure 6C***). Based on these observations, we excluded FoxO1 as a potential downstream target due to its repression role in Tfh cell differentiation (***Stone et al., 2015***). AKT also activates mTORC1, a positive regulator for Tfh cell development (***Zeng et al., 2016***), and in line with the loss of AKT activation, mTORC1 activity was significantly decreased with the ablation of PDK1, as indicated by impaired S6 phosphorylation and reduced Hif1α expression (***Figure 6C***). Taken together, we concluded PDK1-dependent AKT activation is essential for Tfh cell commitment.

Previous studies have revealed AKT phosphorylates and inactivates GSK3β, which then negatively controls β-catenin/TCF1 axis (***Cross et al., 1995***; ***Zhao et al., 2010***). Consistent with decreased p-AKT, phosphorylation of GSK3β was remarkably reduced in PDK1-deficient Tfh cells (***Figure 6C***). Moreover, expression level of TCF1 was much lower in PDK1-null Tfh cells than that of WT cells (***Figure 6C***). Decreased GSK3β phosphorylation in PDK1-deficient Tfh cells caused enhanced GSK3β activity (***Figure 6C***), which was accounted for impaired TCF1 level. It has recently reported that mTORC1-mediated STAT3 phosphorylation induced TCF1 expression in follicular regulatory helper (Tfr) cells (***Xu et al., 2017***). Similarly, we also observed decreased phosphorylation of STAT3 at Ser727 in PDK1-deficient Tfh cells (***Figure 6C***). These analyses collectively suggested that PDK1 may promote Tfh cell differentiation via both mTORC1- and mTORC2-dependent expression of TCF1. To validate this, WT or *Pdk1*$^{fl/fl}$::*Rosa26*^{CreER}::SMARTA cells transduced with TCF1 overexpressing retrovirus plasmid or empty vector (EV) were adoptively transferred into B6.SJL recipients, followed by Tamoxifen treatment and LCMV infection. On 8 dpi, EV-infected *Pdk1*$^{fl/fl}$::*Rosa26*^{CreER}::SMARTA CD4^{+} T cells remained defects in the generation of Tfh cells compared with WT cells, while TCF1 retrovirus promoted differentiation of *Pdk1*$^{fl/fl}$::*Rosa26*^{CreER}::SMARTA CD4^{+} T cells into Tfh cells (***Figure 6D***, ***Figure 6—figure supplement 1B***). In addition, the cell numbers of *Pdk1*$^{fl/fl}$::*Rosa26*^{CreER} Tfh cells were partially rectified by TCF1 (***Figure 6E***). Moreover, overexpression of a constitutive active form of STAT3 (STAT3-CA) could also rectify the defective Tfh cells in the absence of PDK1 (***Figure 6D,E***, ***Figure 6—figure supplement 1B***). Besides, we also found forced expression of Bcl-6 or CXCR5 could partially restore the defective Tfh cell differentiation of PDK1-deficient CD4^{+} T cells (***Figure 6D,E***, ***Figure 6—figure supplement 1B***). Collectively, our data demonstrated that TCF1 serves as one of critical regulators downstream of PDK1 in promoting Tfh cell differentiation.

Discussion

The factors regulating Tfh cell differentiation, migration, and function are still being illustrated. Here, we focused on exploring the role of kinase PDK1 in the regulation of Tfh cell differentiation and

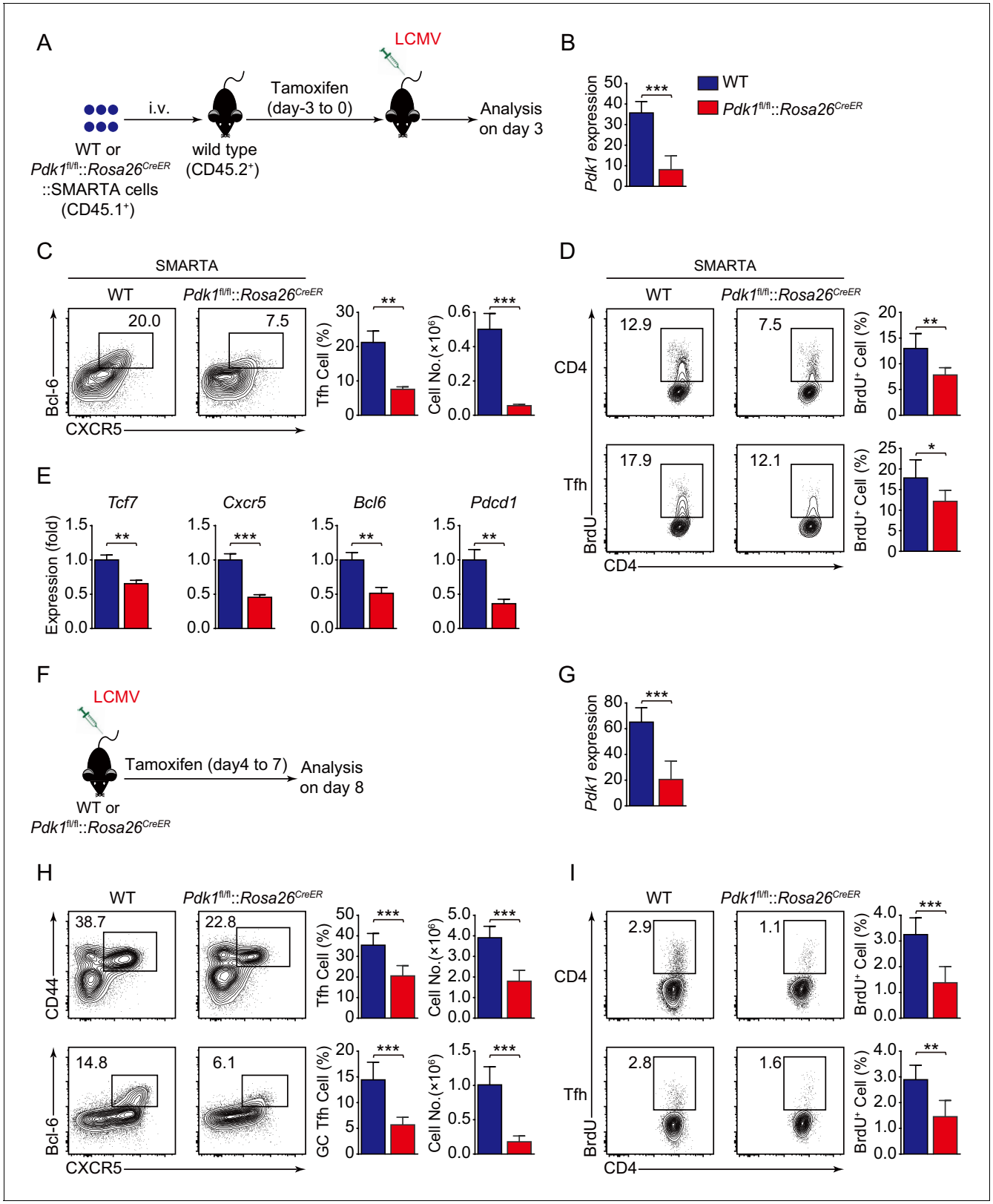

Figure 4. PDK1 is required for both early differentiation and late maintenance of Tfh cells. (**A**) Schematic of the SMARTA cell transfer system used for characterization of early Tfh cell commitment. SMARTA CD4$^+$ T cells from *Pdk1*$^{fl/fl}$::*Rosa26*^{CreER}::SMARTA mice were transferred into C57BL/6J (CD45.2$^+$) host mice, followed by Tamoxifen treatment for four consecutive days, LCMV infection, and analyzed on 3 dpi. (**B**) Quantitative RT-PCR analysis of *Pdk1* abundance in donor-derived CXCR5$^+$ Tfh cells from recipients on 3 dpi as in (**A**) (n = 6). (**C**) Flow cytometry analysis of Bcl-6$^+$CXCR5$^+$

Figure 4 continued on next page

Figure 4 continued

Tfh cells gated on SMARTA CD4$^+$ T cells from recipients on 3 dpi with representative contour plots and cumulative data (n = 3). (**D**) Contour plots represents BrdU$^+$ cells gated on donor-derived activated CD4$^+$ T cells (top panel) and CXCR5$^+$ Tfh cells (bottom panel) from WT and *Pdk1*$^{fl/fl}$::*Rosa26*^{CreER}::SMARTA mice on 3 dpi. Cumulative data on frequency of BrdU$^+$ cells are shown on the right (*n* = 6). (**E**) Quantitative RT-PCR analysis of selected genes in donor-derived CXCR5$^+$ Tfh cells from recipients as in (**A**) (n = 3). (**F**) Schematic of the Tamoxifen-induced deletion system used for characterization of late Tfh cell differentiation. WT and *Pdk1*$^{fl/fl}$::*Rosa26*^{CreER} mice were treated with Tamoxifen from day 4 to day 7 post-LCMV infection and analyzed on 8 dpi. (**G**) Quantitative RT-PCR analysis of *Pdk1* abundance in Tfh cells from WT and *Pdk1*$^{fl/fl}$::*Rosa26*^{CreER} mice on 8 dpi as in (**F**) (n $\geq$ 5). (**H**) Flow cytometry analysis of CD44$^+$CXCR5$^+$ Tfh cells (top panel) gated on CD4$^+$ T cells and Bcl-6$^+$CXCR5$^+$ GC Tfh cells (bottom panel) gated on CD44$^+$CD62L$^-$CD4$^+$ T cells on 8 dpi with representative contour plots and cumulative data (n $\geq$ 5). (**I**) Contour plots represents BrdU$^+$ cells gated on activated CD4$^+$CD44$^+$ T cells (top panel) and CD44$^+$CXCR5$^+$ Tfh cells (bottom panel) from WT and *Pdk1*$^{fl/fl}$::*Rosa26*^{CreER} mice on 8 dpi. Cumulative data on frequency of BrdU$^+$ cells are shown on the right (n $\geq$ 5). Data are representative of at least three independent experiments (**B–C, E, G–H**) or pooled from two independent experiments (**D**). Error bars represent SD. *p<0.05, **p<0.01, and ***p<0.001 (Student's t-test).
The online version of this article includes the following source data and figure supplement(s) for figure 4:

Source data 1. PDK1 is essential for Tfh cell differentiation at both early and late stages.
Figure supplement 1. Detection of apoptosis of activated CD4$^+$ T cells and Tfh cells.
Figure supplement 1—source data 1. Analysis of apoptosis of CD4 T and Tfh cells.

effector function. The generation of Tfh cells was severely compromised in PDK1-deficient mice upon acute LCMV infection and KLH immunization. Correspondingly, the GC responses were also impaired as a consequence of defective Tfh cells. BM chimera results further revealed PDK1 controls Tfh cells in a cell-intrinsic fashion. By using different mice models, we validated that PDK1 is essential for both early expansion and late maintenance of Tfh cells. Taken together, these data support the notion that PDK1 is critical for the development and B-cell helper function of Tfh cells.

CD28 and ICOS are two key costimulatory receptors expressed by Tfh cells, both of which activate PI3Kδ and are essential for Tfh cell differentiation (***Preite et al., 2018b***). Previous study indicated that ICOS-dependent PI3K signal exerts nonredundant function in the generation of Tfh cells (***Gigoux et al., 2009***). By using GSEA and flow cytometry assay, we observed that ICOS functioned as upstream activator of PDK1 in CD4$^+$ T cells. Moreover, we found that Tfh cells exhibited higher expression of PDK1 than Th1 cells and naïve CD4$^+$ T cells. These results collectively suggested that ICOS-dependent PDK1 activity is pivotal for Tfh cells.

The PI3K-AKT signaling pathway is activated by various cell-surface receptors that are crucial for Tfh cell differentiation and function. It is well elaborated that PI3K is a critical component of pathway driving Tfh cell differentiation and GC formation supported by data from PI3K-targeting mice as well as mice and humans expressing activating mutants (***Rolf et al., 2010***; ***Preite et al., 2018a***; ***Preite et al., 2018b***; ***Lucas et al., 2014***). Activation of PI3K facilitates the recruitment of PDK1 and AKT to the plasma membrane through their PH domains, which enables phosphorylation of T308 within the catalytic domain of AKT. To be fully activated, a second crucial residue (S473) located in a hydrophobic motif within AKT's regulatory domain must be phosphorylated by protein kinases like mTORC2 (***Fayard et al., 2010***). mTORC2-deficient mice exhibited severely impaired Tfh cells by activating Tfh cell repressor FoxO1 expression (***Zeng et al., 2016***; ***Hao et al., 2018***), and we observed the phenotypes of *Pdk1*$^{fl/fl}$::*Cd4*-Cre cells almost recapitulated the defects of mTORC2-deficient Tfh cells. mTORC2-deficient T cells exhibited decreased phosphorylation of p-AKT at Ser473 (***Zeng et al., 2016***), whereas, in our experimental system, we found a reduction of both phosphorylated T308 and S473 levels in PDK1-deficient Tfh cells, similar phenomena were also observed in PDK1-null B cells (***Venigalla et al., 2013***). Meanwhile, we observed a reduction of phosphorylated FoxO1/3a and basal FoxO1 levels, which is a downstream molecule of AKT. These results suggested that PDK1-AKT-FoxOs signaling may not be responsible for defective Tfh cells in PDK1-null mice, as FoxO1 is a negative regulator for Tfh cell formation (***Stone et al., 2015***). In addition, the level of phosphorylated S6 was severely decreased in PDK1-deficient Tfh cells, indicating impaired mTORC1 pathway in the absence of PDK1. Compromised mTORC1 activity in turn attenuates protein synthesis and cell proliferation, which are essential for Tfh cell differentiation (***Zeng et al., 2016***). Meanwhile, we found the expression of both *Hif1a* mRNA and Hif1α protein was significantly decreased in PDK1-deficient Tfh cells, which may also contribute to the defective phenotype as loss of Hif1α in CD4$^+$ T cells impairs Tfh cell differentiation (***Cho et al., 2019***;

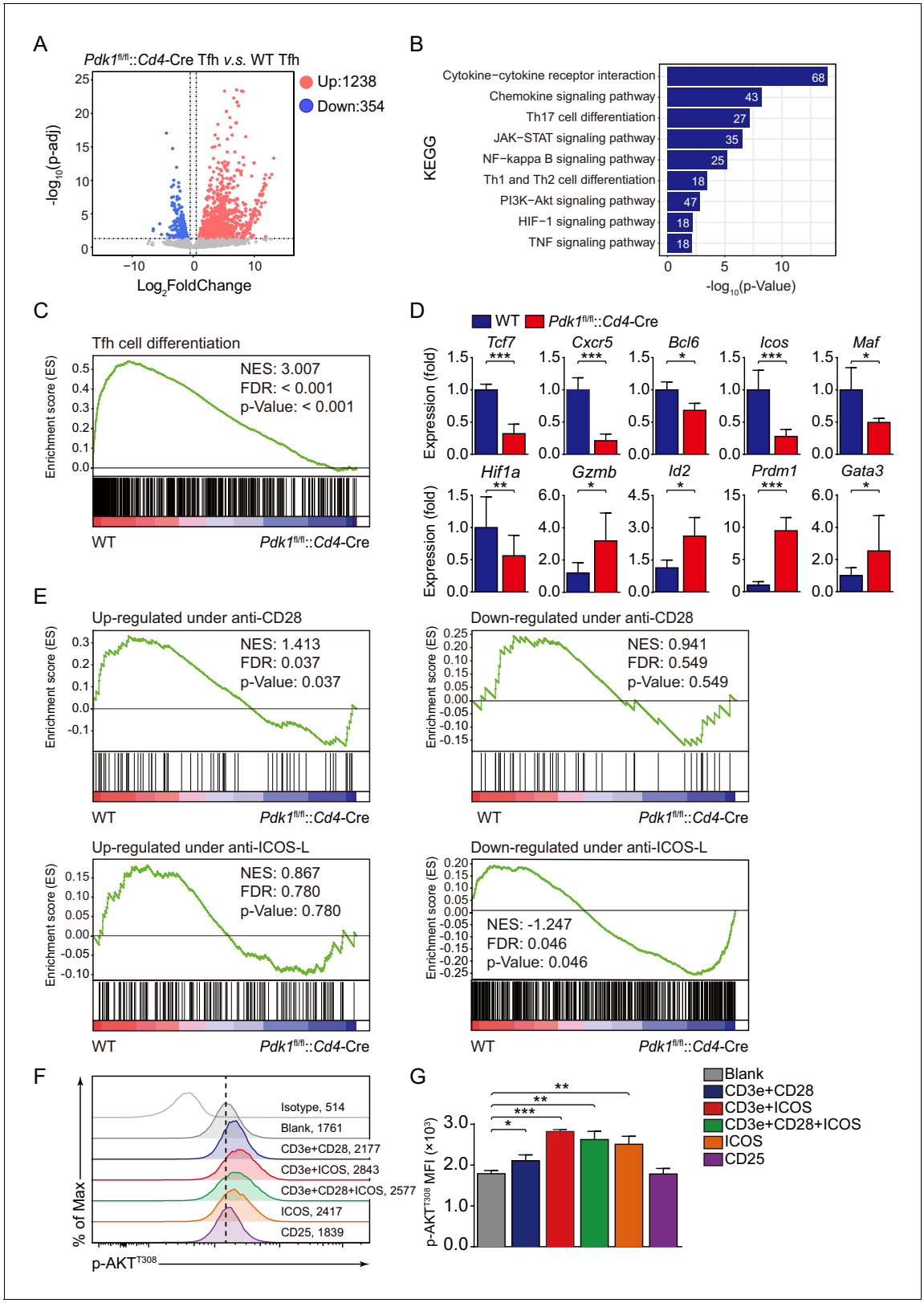

Figure 5. ICOS-dependent PDK1 promotes transcriptional program for Tfh cells. (**A**) RNA-seq analysis of *Pdk1*$^{fl/fl}$::*Cd4*-Cre or WT Tfh cells sort-purified on 8 dpi. Volcano plot shows genes upregulated (red) or downregulated (blue) in *Pdk1*$^{fl/fl}$::*Cd4*-Cre Tfh cells compared with WT cells. (**B**) KEGG pathway analysis of differentially expressed genes in *Pdk1*$^{fl/fl}$::*Cd4*-Cre Tfh cells relative to their expression in WT Tfh cells. (**C**) GSEA of the Tfh cell gene signature in *Pdk1*$^{fl/fl}$::*Cd4*-Cre Tfh cells relative to their expression in WT Tfh cells. (**D**) Quantitative RT-PCR analysis of selected genes in *Pdk1*$^{fl/fl}$::*Cd4*-

Figure 5 continued on next page

Figure 5 continued

Cre and WT Tfh cells. Relative expression was normalized to WT cells (n ≥ 4). (**E**) GSEA of 'Up-regulated under anti-CD28', 'Down-regulated under anti-CD28', 'Up-regulated under anti-ICOS-L', and 'Down-regulated under anti-ICOS-L' gene sets in WT and *Pdk1*$^{fl/fl}$::*Cd4*-Cre Tfh cells. (**F, G**) Flow cytometry analysis of p-AKT^{T308} level on CD4^{+} T cells from WT SMARTA cells, cultured in medium without any stimulus (blank), or stimulated with anti-CD3e + anti-CD28, anti-CD3e + anti-ICOS, anti-CD3e + anti-CD28 + anti-ICOS, anti-ICOS, and anti-CD25. Representative histogram plot and cumulative data are shown in (**F**) and (**G**), respectively (n = 3). Data are representative of at least two independent experiments (**D, F, G**). Error bars represent SD. *p<0.05, and ***p<0.001 (Student's t-test).

The online version of this article includes the following source data for figure 5:

Source data 1. ICOS-dependent PDK1 activity regulates Tfh cell transcriptional files.

He et al., 2019). These results collectively indicated that PDK1-dependent downstream molecular pathways are indispensable for Tfh cell biology.

Transcription factor TCF1 is expressed at an extremely high level in Tfh cells post-viral infection and exerts crucial roles in generation, maintenance, and effector functions of Tfh cells by repressing *Prdm1* and *Il2ra* and promoting *Bcl6* expression (***Shao et al., 2019***; ***Wu et al., 2015***; ***Choi et al., 2015***; ***Xu et al., 2015***). It has been proposed that β-catenin, a coactivator of TCF1 that is negatively regulated by p-GSK3β, linking PI3K-AKT and TCF1 (***Yang et al., 2016***; ***Zhou et al., 2010***). Besides, it has been reported that mTORC1 controls TCF1 expression in Tfr cells by phosphorylated STAT3 (***Xu et al., 2017***). Correspondingly, we found both the p-GSK3β^{S9} and p-STAT3^{S727} levels were significantly decreased in PDK1-deficient Tfh cells. Furthermore, PDK1-null Tfh cells showed both impaired *Tcf7* mRNA and TCF1 protein level. Reconstituting PDK1-deficient CD4^{+} T cells with TCF1 rectifies their defects in the generation of Tfh cells. Moreover, forced expression of STAT3-CA (constitutive active form of STAT3) could restore the Tfh cell numbers of PDK1-deficient mice. These observations collectively suggested that PDK1-dependent TCF1 expression contributes to Tfh cell formation.

In summary, the role of PDK1 in Tfh cell differentiation was extensively investigated in the current study. Our data further suggested PDK1 activates AKT in Tfh cells via phosphorylating both Thr308 and Ser473 residues. On the one side, p-AKT in turn activates mTORC1, and mTORC1 subsequently drives protein synthesis and Hif1α expression and supports TCF1 expression by p-STAT3 to sustain Tfh cell differentiation. On the other side, p-AKT also suppresses GSK3β activity and ultimately promotes TCF1 expression (***Figure 7***). Therefore, our study uncovers PDK1 as a critical regulator for Tfh cell development for both early expansion and late maintenance by mainly modulating TCF1 expression.

Materials and methods

Mice

Pdk1$^{fl/fl}$ mice have been described before (***Lawlor et al., 2002***). *Cd4*-Cre, *Rosa26*^{CreER}, and C57BL/6J (CD45.1 and CD45.2) mice were purchased from the Jackson Laboratory. SMARTA mice (specific for LCMV glycoprotein amino acids 66–77 presented by I-A^{b}) have been described (***Oxenius et al., 1998***) and were crossed to *Pdk1*$^{fl/fl}$::*Rosa26*^{CreER} to generate *Pdk1*$^{fl/fl}$::*Rosa26*^{CreER}::SMARTA mice. All animals were on a C57BL/6J genetic background and used at 6–12 weeks of age. All animal experiments were performed according to protocols approved by the Institutional Animal Care and Use Committee at China Agricultural University.

LCMV infection and KLH immunization

For acute viral infection model, mice were infected intraperitoneally (i.p.) with 2 × 10^{5} pfu (plaque-forming units) of LCMV Armstrong strain in plain DMEM. For KLH immunization model, mice were immunized i.p. with 200 μg of KLH (1 mg/ml, Sigma–Aldrich) emulsified in CFA (1 mg/ml, Sigma–Aldrich). Eight days post-infection or immunization, the mice were sacrificed and splenocytes were examined.

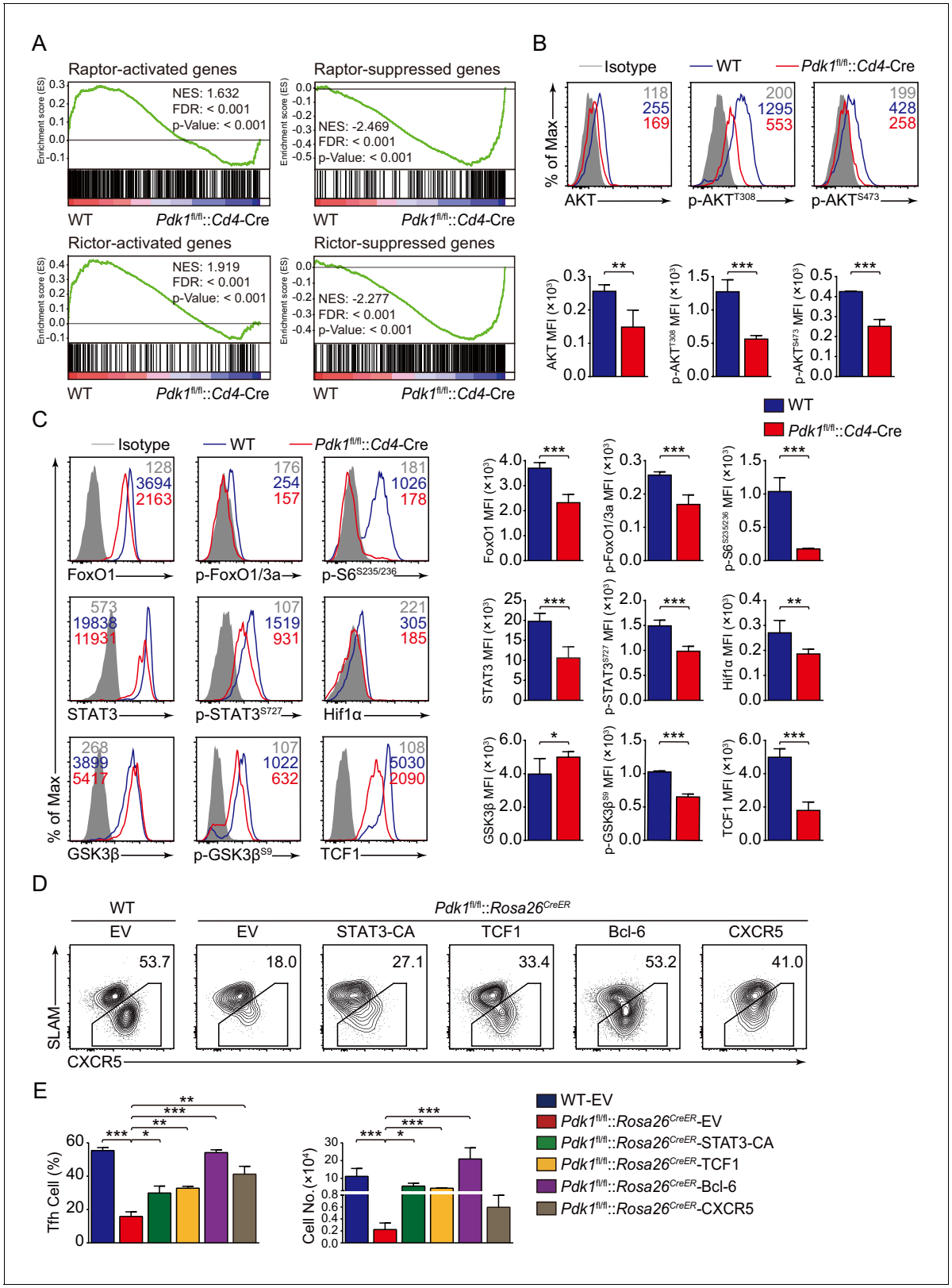

Figure 6. PDK1 deficiency impaired Tfh cell differentiation via mTORC1 and mTORC2 signal-dependent TCF1 expression. (**A**) GSEA of 'Raptor-activated genes', 'Raptor-suppressed genes', 'Rictor-activated genes', and 'Rictor-suppressed genes' gene sets in WT and *Pdk1*$^{fl/fl}$::*Cd4*-Cre Tfh cells. (**B**) Flow cytometry analysis of AKT, p-AKT^{T308}, and p-AKT^{S473} levels on *Pdk1*$^{fl/fl}$::*Cd4*-Cre and WT Tfh cells on 8 dpi by flow cytometry with representative histograms and quantification data (n = 4). (**C**) Flow cytometry analysis of FoxO1, p-FoxO1/3a, STAT3, p-STAT3^{S727}, Hif1α, p-S6, GSK3β,

Figure 6 continued on next page

Figure 6 continued

p-GSK3β^{S9}, and TCF1 levels on *Pdk1*$^{fl/fl}$::*Cd4*-Cre and WT Tfh cells on 8 dpi by flow cytometry with representative histograms and quantification data ($n \geq 4$). (**D, E**) Flow cytometry analysis of Tfh populations from recipients adoptively transferred with STAT3-CA, TCF1, Bcl-6, or CXCR5 retrovirus-infected SMARTA cells on 8 dpi by flow cytometry with representative contour plots and cumulative data in (**D**) and (**E**), respectively ($n \geq 3$). Data are representative of at least two independent experiments. Error bars represent SD. *p<0.05, **p<0.01, and ***p<0.001 (Student's t-test).
The online version of this article includes the following source data and figure supplement(s) for figure 6:

Source data 1. PDK1 regulates Tfh cell differentiation via mTORC1 and mTORC2 signal-dependent TCF1 expression.
Figure supplement 1. Analysis of p-PKCζ/λ level in Tfh cells and detection of overexpression level of relative genes in primed CD4$^+$ cells via retrovirus transduction.
Figure supplement 1—source data 1. Analysis of p-PKCζ/λ level and validation of overexpression efficiency.

Flow cytometry

Single-cell suspensions were prepared from the spleens or peripheral blood for surface or intracellular staining. The fluorochrome-conjugated antibodies were used as follows: anti-CD4 (RM4-5), anti-CD25 (PC61), anti-CD44 (IM7), anti-CD45.1 (A20), anti-CD45.2 (104), anti-CD62L (MEL-14), anti-CD45R (RA3-6B2), anti-PD-1 (J43), anti-TCR Vα2 (B20.1), anti-IFNγ (XMG1.2), anti-IL-4 (11B11), anti-Foxp3 (FJK-16S) (from Thermo Fisher Scientific), anti-CD138 (281-2), anti-Fas (Jo2), anti-Bcl-6 (K112-91), anti-IL-17a (TC11-18H10) (from BD Biosciences), anti-SLAM (TC15-12F12.2), anti-ICOS (C398.4A)

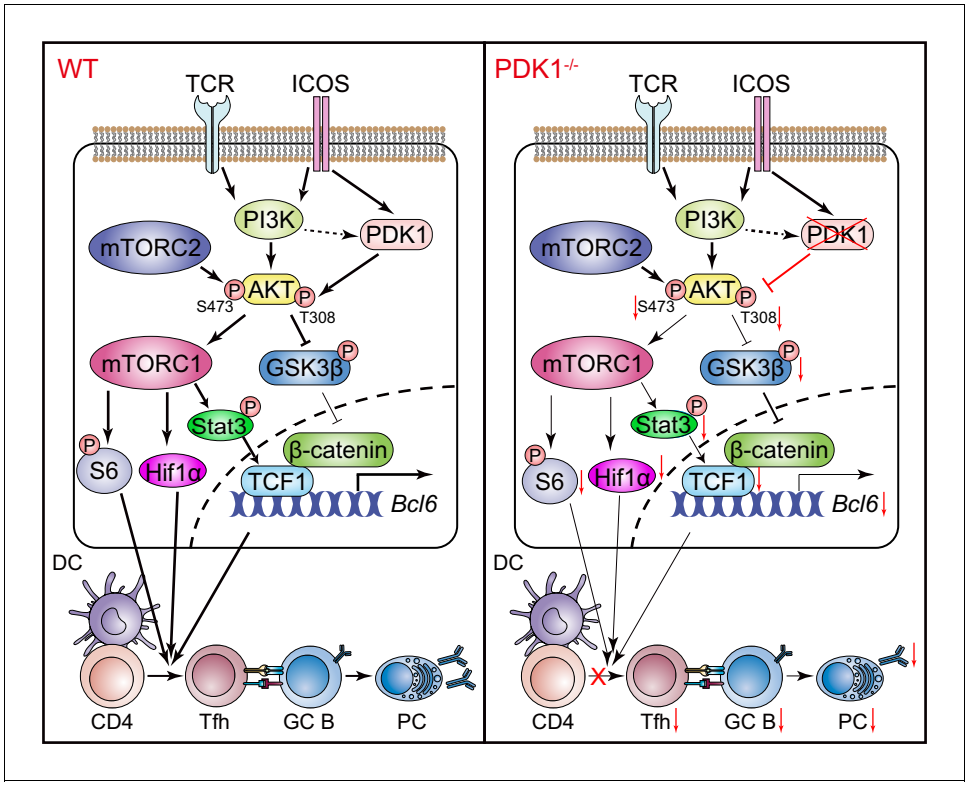

Figure 7. Working model of PDK1 in regulating Tfh cell differentiation. Left panel: In PDK1-sufficient cells, AKT gets activated by phosphorylation at Thr308 and Ser473. p-AKT activates mTORC1, and mTORC1 further phosphorylates S6 and supports Hif1α expression, promoting protein synthesis, proliferation, and metabolization. mTORC1 also phosphorates STAT3 to induce TCF1 expression. In addition, p-AKT also guards TCF1 activity through the inactivation of GSK3β, an inhibitor of TCF1 and β-catenin. Enhanced TCF1 contributes to Tfh cell differentiation, GC responses, and humoral immunity. Right panel: In PDK1-deficient cells, AKT remains inactivated by loss of phosphorylation at Thr308 and Ser473, which contributes to impaired mTORC1 activity and activities of downstream molecules, inducing p-STAT3-dependent TCF1 expression. In addition, inactivation of p-AKT leads to compromised p-GSK3β, resulting in increased GSK3β activity and subsequently inhibition on TCF1 level. Decreased TCF1 leads to impaired Tfh cell differentiation, GC responses, and humoral immunity.

(from BioLegend); PNA (Cat # FL-1071) (from Vector Laboratories), anti-TCF1 (C63D9), anti-PDK1 (Cat # 3062), anti-FoxO1 (C29H4), anti-Hif1α (D1S7W), anti-p-AKT^{T308} (D25E6), anti-p-AKT^{S473} (D9E), anti-p-STAT3^{S727} (Cat # 9134), anti-p-GSK3β^{S9} (D85E12), anti-p-S6$^{S235/236}$ (D57.2.2E), anti-p-FoxO1/3a (Cat # 9464), anti-p-PKCζ/λ (Cat # 9378) (from Cell Signaling Technology), and anti-AKT (Cat # AA326) and anti-GSK3β (Cat # AF1543) (from Beyotime Biotechnology). For detection of CXCR5, a three-step staining protocol was used with unconjugated anti-CXCR5 (2G8; BD Biosciences) as described before (**Yao et al., 2018**). For detection of Bcl-6, TCF1, and Foxp3, surface-stained cells were fixed and permeabilized with the Foxp3 Transcription Factor Staining Buffer Set (Thermo Fisher Scientific), followed by incubation with corresponding fluorochrome-conjugated antibodies. For the analysis of cytokine production, splenocytes well stimulated in vitro with PMA (Sigma–Aldrich) and Ionomycin (Sigma–Aldrich) at 37˚C for 5 hr, then the cells were fixed and permeabilized with Cytofix/Cytoperm Fixation/Permeabilization Solution Kit (554714, BD Biosciences). For detection of phosphorylated proteins, stimulated cells were immediately fixed with Phosflow Lyse/Fix buffer (558049, BD Biosciences), followed by permeabilization with Phosflow Perm buffer I (557885, Biosciences), incubation with corresponding primary unconjugated antibodies and sequential staining with fluorochrome-conjugated donkey anti-rabbit IgG (poly4064; BioLegend). Flow cytometry data were collected on an LSRFortessa or a FACSVerse (BD Biosciences) and were analyzed with FlowJo software (TreeStar). The surface-stained cells were sort-purified on a FACSAria II (BD Biosciences).

Adoptive transfer

For the adoptive transfer experiments, a total of 5 × 10^6 (analysis on day 3) SMARTA CD4$^+$ T cells from WT or *Pdk1*$^{fl/fl}$::*Rosa26*^{CreER}::SMARTA mice were adoptively transferred to congenic recipient mice. The recipient mice then received daily oval gavage with 2 mg of tamoxifen (Sigma–Aldrich) diluted in corn oil for 4 days, followed by intravenously (i.v.) infection with 2 × 10^6 pfu of LCMV Armstrong. On 8 dpi, the recipient mice were sacrificed, and the splenocytes were analyzed by flow cytometry.

Retroviral transduction pMIG-*Tcf7*, pMIG-*Bcl6*, pMIG-*Cxcr5*, MIG-*Stat3-CA*, and pMIG-R1 retroviral vectors were used to produce retrovirus from the HEK293 T cell lines. *Pdk1*$^{fl/fl}$::*Rosa26*^{CreER} or WT SMARTA mice were i.v. injected with 200 μg of GP61 peptide (GLKGPDIYKGVYQFKSVEFD) to prime the SMARTA CD4$^+$ T cells. Sixteen hours later, the splenic CD4$^+$ T cells were isolated and infected by spinofection at 2100 rpm, 32℃ for 90 min, and then cultured overnight in the presence of mIL-2 (20 ng/ml, PEPROTECH) and GP61 peptide (250 nM). The spinofection was repeated next day, and a total of 0.5 to 1 × 10^6 retrovirally infected SMARTA CD4$^+$ T cells (CD45.2$^+$) were i.v. transferred into CD45.1$^+$ recipients. The recipient mice received daily oval gavage with 2 mg of tamoxifen (Sigma–Aldrich) diluted in corn oil for 3 days, followed by i.p. infected with 2 × 10^5 pfu of LCMV Armstrong. The recipient mice were sacrificed, and spleens were examined 8 dpi.

BM chimeras

BM chimeras were generated as previously described (**Liu et al., 2019**). Briefly, 2 × 10^6 BM cells of a 1:1 mixture from *Pdk1*$^{fl/fl}$::*Cd4*-Cre or WT donor mice (CD45.2$^+$) and CD45.1$^+$CD45.2$^+$ competitor mice were i.v. transferred into lethally irradiated (7.5 Gray each) wild-type CD45.1$^+$CD45.2$^+$ recipients. After 9 weeks reconstitution, recipient mice were infected with LCMV Armstrong. The recipient mice were sacrificed and spleens were examined 8 dpi.

Enzyme-linked immunosorbent assay (ELISA)

ELISA to detect LCMV-specific IgG was performed as previously described (**Yao et al., 2018**). Briefly, Nunc MaxiSorp flat-bottom 96-well microplates (Thermo Fisher Scientific) were coated with LCMV-BHK21 lysates overnight. Plates were blocked with phosphate-buffered saline (PBS) + 0.05% Tween-20 + 1% BSA (PBST-B) for 30 min at room temperature. After washing, serum samples were added in serial dilution by PBST and incubated for 60 min at room temperature followed washing by PBST. Next, horseradish peroxidase-conjugated goat-anti-mouse IgG secondary antibody (Bethyl Laboratories) was added at 1:5000 in PBST-B for 60 min at room temperature. The LCMV-specific IgG was detected by coupling with TMB substrate (BioLegend). The absorbance at 450 nm was read on a microplate reader (TECAN).

Immunofluorescence staining

Spleens from mice infected with LCMV Armstrong were snap-frozen in OCT medium (Sakura Finetek) by liquid nitrogen. Ten-micrometer-thick sections were cut using a Cryostat Microtome System. Tissue sections were fixed with cold acetone for 30 min at −20˚C, blocked with 5% BSA, and stained with biotin-PNA (Vector Laboratories), APC-labeled anti-IgD (11–26 c.2a; Thermo Fisher Scientific), and BV510-labeled anti-CD4 (RM4-5; BD Biosciences), followed by FITC-labeled streptavidin (Thermo Fisher Scientific). After each step, the slides were washed at least three times with PBS. Sections were fixed and mounted with an antifade kit (P0123, Beyotime Biotechnology) and then examined using a confocal fluorescence microscope. The images were processed with Imaris and Image J software.

Detection of PDK1 activity

For detection of PDK1 activity, WT SMARTA mice were i.v. injected with 200 μg of GP61 peptide to prime the SMARTA $CD4^+$ T cells. Sixteen hours later, the splenic were isolated and were first stained with surface markers and then were stimulated with anti-CD3e (2 μg/ml, 145–2 C11; BioXcell), anti-CD28 (1 μg/ml, BE0015, BioXcell), anti-ICOS (2 μg/ml, C398.4A, Biolegend), or anti-CD25 (2 μg/ml, BE0012, BioXcell) at 37˚C, 5% CO_2 for 1 hr. Stimulated cells were immediately fixed with Phosflow Lyse/Fix buffer (558049, BD Biosciences), incubated with rabbit anti-p-AKT^{T308} (D25E6; Cell Signaling Technology), and sequential stained with fluorochrome-conjugated donkey anti-rabbit IgG (poly4064; BioLegend).

Proliferation and apoptosis assays

For cell proliferation assay, the mice with indicated genotype were given 2 mg of BrdU i.p. 3 hr before sacrifice. Cells were first stained with surface markers and then were fixed and permeabilized with Cytofix/Cytoperm Fixation/Permeabilization Solution Kit (554714, BD Biosciences). Next, cells were intracellularly stained with anti-BrdU antibody using the BrdU Flow Kit (BD Biosciences) according to manufacturer's introduction. For apoptosis assays, the cells were first stained with surface markers, followed by staining with Caspase-3 (Thermo Fisher Scientific) at 37℃ for 1 hr.

Transwell migration chemotaxis assay

On 8 dpi, total splenocyte samples from WT and *Pdk1*$^{fl/fl}$::*Cd4*-Cre mice were subjected to depletion of cells that were positive for lineage markers (Lin^+ cells) using biotin-conjugated antibodies (anti-CD8 [53–6.7], anti-B220 [RA3-6B2], anti-CD11c [N418], anti-Gr.1 [RB6-8C5], anti-TER119 [TER-119], and anti-NK1.1 [PK136], all from Thermo Fisher Scientific) coupled with the BeaverBeads Mag Streptavidin (Cat # 22305; Beaver). The Lin^- cells were then surface stained with anti-CD4, anti-CD44, and anti-CXCR5 to identify Tfh cells. Next, 4×10^5 Tfh cells from WT or *Pdk1*$^{fl/fl}$::*Cd4*-Cre mice were loaded into the upper chamber of a 24-well transwell plate (5 μm pore, Corning), and 600 μl of chemotaxis medium supplemented with or without the 1 μg/ml of CXCL13 (583906, Biolegend) was added to the lower chamber. The cells were allowed to migrate for 3 hr in a 5% CO_2 incubator at 37˚C. Then, all the migrated cells were collected from the lower chamber, and the numbers of migrated Tfh cells were determined by flow cytometry. Based on the absolute number of Tfh cells, the 'net migration (% of input)' was calculated as follows: Net migration (% of input) = (# of migrated Tfh cells to CXCL13 − # of migrated Tfh cells in the absence of CXCL13)/(# of Tfh cells in the input sample).

RNA-seq and data processing

Pdk1$^{fl/fl}$::*Cd4*-Cre and WT mice were infected with LCMV Armstrong, and on 8 dpi, $CD4^+CD44^+$-$SLAM^{lo}$ Tfh cells were sorted and total RNA was extracted. Two biological replicates were obtained for both genotypes of mice and used for RNA-seq analysis. Read quality was checked for each sample using FastQC (v0.11.5). Reads were then mapped to the reference genome (mm9) using TopHat (v2.1.1). Raw alignment counts were calculated with R/Bioconductor package GenomicRanges (v1.36.1). Differential expression analysis was performed with DESeq2 (v1.24.0) from the counts. RPKM was calculated, and upregulated or downregulated genes in *Pdk1*$^{fl/fl}$::*Cd4*-Cre Tfh cells were identified by $|\log_2 FoldChange| \geq 0.5$ and false discovery rate<0.05.

Quantitative RT-PCR

Tfh cells were sorted from the spleens of *Pdk1*$^{fl/fl}$::*Cd4*-Cre and WT mice on day 8 post-LCMV Armstrong infection. Total RNA was extracted and reverse-transcribed, and target gene transcripts were measured with quantitative PCR. The primers were listed in **Key Resources Table** above.

Gene set enrichment analysis

GSEA was performed with GSEA software (version 3.0) with default settings from the Broad Institute and used to determine enrichment of gene sets in WT or *Pdk1*$^{fl/fl}$::*Cd4*-Cre Tfh cells. The gene set of 'Tfh cell differentiation', 'Up-regulated under anti-CD28', 'Down-regulated under anti-CD28', 'Up-regulated under anti-ICOS-L', 'Down-regulated under anti-ICOS-L', 'Raptor-activated genes', 'Raptor-suppressed genes', 'Rictor-activated genes', and 'Rictor-suppressed genes' were collected from previously studies (***Zeng et al., 2016***; ***Hao et al., 2018***; ***Riley et al., 2002***; ***Künzli et al., 2020***).

Statistical analysis

The statistical significance of differences between groups was determined using two-tailed, unpaired Student's t-test with 95% confidence intervals unless otherwise indicated and GraphPad Prism software (version 8.0). Differences with p-values$\geq$0.05 were considered non-significant (NS). p-values<0.05 were considered significant (*p<0.05; **p<0.01; ***p<0.001).

Additional information

Funding

Funder	Grant reference number	Author
National Key Research and Development Program of China	2017YFA0104401	Shuyang Yu
National Natural Science Foundation of China	31970831	Shuyang Yu
National Natural Science Foundation of China	31630038	Shuyang Yu
National Natural Science Foundation of China	31571522	Shuyang Yu
National Natural Science Foundation of China	31422037	Shuyang Yu
National Natural Science Foundation of China	81770105	Weiping Yuan
State Key Laboratory of Agrobiotechnology, China Agricultural University	2019SKLAB6-6	Shuyang Yu
State Key Laboratory of Agrobiotechnology, China Agricultural University	2019SKLAB6-7	Shuyang Yu
State Key Laboratory of Agrobiotechnology, China Agricultural University	2018SKLAB6-30	Shuyang Yu

The funders had no role in study design, data collection and interpretation, or the decision to submit the work for publication.

Author contributions

Zhen Sun, Software, Formal analysis, Investigation, Visualization, Methodology, Project administration; Yingpeng Yao, Software, Validation, Investigation, Visualization, Writing - original draft, Writing - review and editing; Menghao You, Software, Investigation, Methodology, Writing - original draft, Writing - review and editing; Jingjing Liu, Formal analysis, Validation, Investigation, Methodology; Wenhui Guo, Formal analysis, Validation, Investigation; Zhihong Qi, Validation, Investigation; Zhao

Wang, Software, Formal analysis, Investigation; Fang Wang, Software, Formal analysis, Validation, Investigation, Methodology; Weiping Yuan, Resources, Formal analysis; Shuyang Yu, Conceptualization, Resources, Supervision, Funding acquisition, Validation, Writing - original draft, Project administration, Writing - review and editing

Author ORCIDs
Zhen Sun http://orcid.org/0000-0001-5380-6831
Yingpeng Yao https://orcid.org/0000-0002-5415-2443
Fang Wang http://orcid.org/0000-0002-2604-4429
Weiping Yuan http://orcid.org/0000-0001-8288-5022
Shuyang Yu https://orcid.org/0000-0002-4686-3296

Ethics
Animal experimentation: This study was performed in strict accordance with the recommendations in the Guide for the Care and Use of Laboratory Animals of the China Agricultural University. All of the animals were handled according to protocols approved by the Institutional Animal Care and Use Committee at China Agricultural University (Ethical approval Number: AW40101202-3-5).

Decision letter and Author response
Decision letter https://doi.org/10.7554/eLife.61406.sa1
Author response https://doi.org/10.7554/eLife.61406.sa2

Additional files
Supplementary files
- Transparent reporting form

Data availability
Sequencing data have been deposited in GEO under accession number GSE154976.

The following dataset was generated:

Author(s)	Year	Dataset title	Dataset URL	Database and Identifier
Yu S	2020	Regulation of Tfh differentiation by PDK1	https://www.ncbi.nlm.nih.gov/geo/query/acc.cgi?acc=GSE154976	NCBI Gene Expression Omnibus, GSE154976

References
Baracho GV, Cato MH, Zhu Z, Jaren OR, Hobeika E, Reth M, Rickert RC. 2014. PDK1 regulates B cell differentiation and homeostasis. *PNAS* **111**:9573–9578. DOI: https://doi.org/10.1073/pnas.1314562111, PMID: 24979759

Baumjohann D, Preite S, Reboldi A, Ronchi F, Ansel KM, Lanzavecchia A, Sallusto F. 2013. Persistent antigen and germinal center B cells sustain T follicular helper cell responses and phenotype. *Immunity* **38**:596–605. DOI: https://doi.org/10.1016/j.immuni.2012.11.020, PMID: 23499493

Bauquet AT, Jin H, Paterson AM, Mitsdoerffer M, Ho IC, Sharpe AH, Kuchroo VK. 2009. The costimulatory molecule ICOS regulates the expression of c-Maf and IL-21 in the development of follicular T helper cells and T_H-17 cells. *Nature Immunology* **10**:167–175. DOI: https://doi.org/10.1038/ni.1690, PMID: 19098919

Cho SH, Raybuck AL, Blagih J, Kemboi E, Haase VH, Jones RG, Boothby MR. 2019. Hypoxia-inducible factors in $CD4^+$ T cells promote metabolism, switch cytokine secretion, and T cell help in humoral immunity. *PNAS* **116**:8975–8984. DOI: https://doi.org/10.1073/pnas.1811702116, PMID: 30988188

Choi YS, Gullicksrud JA, Xing S, Zeng Z, Shan Q, Li F, Love PE, Peng W, Xue HH, Crotty S. 2015. LEF-1 and TCF-1 orchestrate $T_{(FH)}$ differentiation by regulating differentiation circuits upstream of the transcriptional repressor Bcl6. *Nature Immunology* **16**:980–990. DOI: https://doi.org/10.1038/ni.3226, PMID: 26214741

Cross DA, Alessi DR, Cohen P, Andjelkovich M, Hemmings BA. 1995. Inhibition of glycogen synthase kinase-3 by insulin mediated by protein kinase B. *Nature* **378**:785–789. DOI: https://doi.org/10.1038/378785a0, PMID: 8524413

Crotty S. 2011. Follicular helper CD4 T cells (T_{FH}). *Annual Review of Immunology* **29**:621–663. DOI: https://doi.org/10.1146/annurev-immunol-031210-101400, PMID: 21314428

Crotty S. 2014. T follicular helper cell differentiation, function, and roles in disease. *Immunity* **41**:529–542. DOI: https://doi.org/10.1016/j.immuni.2014.10.004, PMID: 25367570

Crotty S. 2019. T follicular helper cell biology: a decade of discovery and diseases. *Immunity* **50**:1132–1148. DOI: https://doi.org/10.1016/j.immuni.2019.04.011, PMID: 31117010

Deenick EK, Chan A, Ma CS, Gatto D, Schwartzberg PL, Brink R, Tangye SG. 2010. Follicular helper T cell differentiation requires continuous antigen presentation that is independent of unique B cell signaling. *Immunity* **33**:241–253. DOI: https://doi.org/10.1016/j.immuni.2010.07.015, PMID: 20691615

Fayard E, Moncayo G, Hemmings BA, Holländer GA. 2010. Phosphatidylinositol 3-kinase signaling in thymocytes: the need for stringent control. *Science Signaling* **3**:re5. DOI: https://doi.org/10.1126/scisignal.3135re5, PMID: 20716765

Fazilleau N, McHeyzer-Williams LJ, Rosen H, McHeyzer-Williams MG. 2009. The function of follicular helper T cells is regulated by the strength of T cell antigen receptor binding. *Nature Immunology* **10**:375–384. DOI: https://doi.org/10.1038/ni.1704, PMID: 19252493

Finlay DK, Rosenzweig E, Sinclair LV, Feijoo-Carnero C, Hukelmann JL, Rolf J, Panteleyev AA, Okkenhaug K, Cantrell DA. 2012. PDK1 regulation of mTOR and hypoxia-inducible factor 1 integrate metabolism and migration of $CD8^+$ T cells. *Journal of Experimental Medicine* **209**:2441–2453. DOI: https://doi.org/10.1084/jem.20112607

Gigoux M, Shang J, Pak Y, Xu M, Choe J, Mak TW, Suh WK. 2009. Inducible costimulator promotes helper T-cell differentiation through phosphoinositide 3-kinase. *PNAS* **106**:20371–20376. DOI: https://doi.org/10.1073/pnas.0911573106, PMID: 19915142

Hao Y, Wang Y, Liu X, Yang X, Wang P, Tian Q, Bai Q, Chen X, Li Z, Wu J, Xie Z, Zhou X, Zhou Y, Yin Z, Wu Y, Ye L. 2018. The kinase complex mTOR complex 2 promotes the follicular migration and functional maturation of differentiated follicular helper $CD4^+$ T Cells During Viral Infection. *Frontiers in Immunology* **9**:1127. DOI: https://doi.org/10.3389/fimmu.2018.01127, PMID: 29875775

He Y, Zhou S, Cao Y, Li Y, Bi Y, Liu Y. 2019. HIF1α-Dependent metabolic signals control the differentiation of follicular helper T cells. *Cells* **8**:1450. DOI: https://doi.org/10.3390/cells8111450

Johnston RJ, Poholek AC, DiToro D, Yusuf I, Eto D, Barnett B, Dent AL, Craft J, Crotty S. 2009. Bcl6 and Blimp-1 are reciprocal and antagonistic regulators of T follicular helper cell differentiation. *Science* **325**:1006–1010. DOI: https://doi.org/10.1126/science.1175870, PMID: 19608860

Künzli M, Schreiner D, Pereboom TC, Swarnalekha N, Litzler LC, Lötscher J, Ertuna YI, Roux J, Geier F, Jakob RP, Maier T, Hess C, Taylor JJ, King CG. 2020. Long-lived T follicular helper cells retain plasticity and help sustain humoral immunity. *Science Immunology* **5**:eaay5552. DOI: https://doi.org/10.1126/sciimmunol.aay5552, PMID: 32144185

Lawlor MA, Mora A, Ashby PR, Williams MR, Murray-Tait V, Malone L, Prescott AR, Lucocq JM, Alessi DR. 2002. Essential role of PDK1 in regulating cell size and development in mice. *The EMBO Journal* **21**:3728–3738. DOI: https://doi.org/10.1093/emboj/cdf387, PMID: 12110585

Leavenworth JW, Verbinnen B, Yin J, Huang H, Cantor H. 2015. A p85α-osteopontin axis couples the receptor ICOS to sustained Bcl-6 expression by follicular helper and regulatory T cells. *Nature Immunology* **16**:96–106. DOI: https://doi.org/10.1038/ni.3050

Liu J, Cui Z, Wang F, Yao Y, Yu G, Liu J, Cao D, Niu S, You M, Sun Z, Lian D, Zhao T, Kang Y, Zhao Y, Xue HH, Yu S. 2019. Lrp5 and Lrp6 are required for maintaining self-renewal and differentiation of hematopoietic stem cells. *The FASEB Journal* **33**:5615–5625. DOI: https://doi.org/10.1096/fj.201802072R

Lucas CL, Kuehn HS, Zhao F, Niemela JE, Deenick EK, Palendira U, Avery DT, Moens L, Cannons JL, Biancalana M, Stoddard J, Ouyang W, Frucht DM, Rao VK, Atkinson TP, Agharahimi A, Hussey AA, Folio LR, Olivier KN, Fleisher TA, et al. 2014. Dominant-activating germline mutations in the gene encoding the PI(3)K catalytic subunit p110δ result in T cell senescence and human immunodeficiency. *Nature Immunology* **15**:88–97. DOI: https://doi.org/10.1038/ni.2771, PMID: 24165795

Nurieva RI, Chung Y, Martinez GJ, Yang XO, Tanaka S, Matskevitch TD, Wang YH, Dong C. 2009. Bcl6 mediates the development of T follicular helper cells. *Science* **325**:1001–1005. DOI: https://doi.org/10.1126/science.1176676, PMID: 19628815

Oxenius A, Bachmann MF, Zinkernagel RM, Hengartner H. 1998. Virus-specific MHC-class II-restricted TCR-transgenic mice: effects on humoral and cellular immune responses after viral infection. *European Journal of Immunology* **28**:390–400. DOI: https://doi.org/10.1002/(SICI)1521-4141(199801)28:01<390::AID-IMMU390>3.0.CO;2-O, PMID: 9485218

Park S-G, Schulze-Luehrman J, Hayden MS, Hashimoto N, Ogawa W, Kasuga M, Ghosh S. 2009. The kinase PDK1 integrates T cell antigen receptor and CD28 coreceptor signaling to induce NF-κB and activate T cells. *Nature Immunology* **10**:158–166. DOI: https://doi.org/10.1038/ni.1687

Preite S, Cannons JL, Radtke AJ, Vujkovic-Cvijin I, Gomez-Rodriguez J, Volpi S, Huang B, Cheng J, Collins N, Reilley J, Handon R, Dobbs K, Huq L, Raman I, Zhu C, Li QZ, Li MO, Pittaluga S, Uzel G, Notarangelo LD, et al. 2018a. Hyperactivated PI3Kδ promotes self and commensal reactivity at the expense of optimal humoral immunity. *Nature Immunology* **19**:986–1000. DOI: https://doi.org/10.1038/s41590-018-0182-3, PMID: 30127432

Preite S, Huang B, Cannons JL, McGavern DB, Schwartzberg PL. 2018b. PI3K orchestrates T follicular helper cell differentiation in a context dependent manner: implications for autoimmunity. *Frontiers in Immunology* **9**:3079. DOI: https://doi.org/10.3389/fimmu.2018.03079, PMID: 30666254

Qin L, Waseem TC, Sahoo A, Bieerkehazhi S, Zhou H, Galkina EV, Nurieva R. 2018. Insights into the molecular mechanisms of T follicular Helper-Mediated immunity and pathology. *Frontiers in Immunology* **9**:9. DOI: https://doi.org/10.3389/fimmu.2018.01884

Riley JL, Mao M, Kobayashi S, Biery M, Burchard J, Cavet G, Gregson BP, June CH, Linsley PS. 2002. Modulation of TCR-induced transcriptional profiles by ligation of CD28, ICOS, and CTLA-4 receptors. *PNAS* **99**:11790–11795. DOI: https://doi.org/10.1073/pnas.162359999, PMID: 12195015

Rolf J, Bell SE, Kovesdi D, Janas ML, Soond DR, Webb LM, Santinelli S, Saunders T, Hebeis B, Killeen N, Okkenhaug K, Turner M. 2010. Phosphoinositide 3-kinase activity in T cells regulates the magnitude of the germinal center reaction. *The Journal of Immunology* **185**:4042–4052. DOI: https://doi.org/10.4049/jimmunol.1001730, PMID: 20826752

Shao P, Li F, Wang J, Chen X, Liu C, Xue HH. 2019. Cutting edge: tcf1 instructs T follicular helper cell differentiation by repressing Blimp1 in response to acute viral infection. *The Journal of Immunology* **203**:801–806. DOI: https://doi.org/10.4049/jimmunol.1900581, PMID: 31300510

Shrestha S, Yang K, Guy C, Vogel P, Neale G, Chi H. 2015. Treg cells require the phosphatase PTEN to restrain TH1 and TF_H cell responses. *Nature Immunology* **16**:178–187. DOI: https://doi.org/10.1038/ni.3076, PMID: 25559258

Stone EL, Pepper M, Katayama CD, Kerdiles YM, Lai CY, Emslie E, Lin YC, Yang E, Goldrath AW, Li MO, Cantrell DA, Hedrick SM. 2015. ICOS coreceptor signaling inactivates the transcription factor FOXO1 to promote tfh cell differentiation. *Immunity* **42**:239–251. DOI: https://doi.org/10.1016/j.immuni.2015.01.017, PMID: 25692700

Tubo NJ, Pagán AJ, Taylor JJ, Nelson RW, Linehan JL, Ertelt JM, Huseby ES, Way SS, Jenkins MK. 2013. Single naive $CD4^+$ T cells from a diverse repertoire produce different effector cell types during infection. *Cell* **153**:785–796. DOI: https://doi.org/10.1016/j.cell.2013.04.007, PMID: 23663778

Venigalla RK, McGuire VA, Clarke R, Patterson-Kane JC, Najafov A, Toth R, McCarthy PC, Simeons F, Stojanovski L, Arthur JS. 2013. PDK1 regulates VDJ recombination, cell-cycle exit and survival during B-cell development. *The EMBO Journal* **32**:1008–1022. DOI: https://doi.org/10.1038/emboj.2013.40, PMID: 23463102

Wu T, Shin HM, Moseman EA, Ji Y, Huang B, Harly C, Sen JM, Berg LJ, Gattinoni L, McGavern DB, Schwartzberg PL. 2015. TCF1 is required for the T follicular helper cell response to viral infection. *Cell Reports* **12**:2099–2110. DOI: https://doi.org/10.1016/j.celrep.2015.08.049, PMID: 26365183

Xu L, Cao Y, Xie Z, Huang Q, Bai Q, Yang X, He R, Hao Y, Wang H, Zhao T, Fan Z, Qin A, Ye J, Zhou X, Ye L, Wu Y. 2015. The transcription factor TCF-1 initiates the differentiation of $T_{(FH)}$ cells during acute viral infection. *Nature Immunology* **16**:991–999. DOI: https://doi.org/10.1038/ni.3229, PMID: 26214740

Xu L, Huang Q, Wang H, Hao Y, Bai Q, Hu J, Li Y, Wang P, Chen X, He R, Li B, Yang X, Zhao T, Zhang Y, Wang Y, Ou J, Liang H, Wu Y, Zhou X, Ye L. 2017. The kinase mTORC1 promotes the generation and suppressive function of follicular regulatory T cells. *Immunity* **47**:538–551. DOI: https://doi.org/10.1016/j.immuni.2017.08.011, PMID: 28930662

Yang M, Li D, Chang Z, Yang Z, Tian Z, Dong Z. 2015. PDK1 orchestrates early NK cell development through induction of E4BP4 expression and maintenance of IL-15 responsiveness. *Journal of Experimental Medicine* **212**:253–265. DOI: https://doi.org/10.1084/jem.20141703

Yang J, Lin X, Pan Y, Wang J, Chen P, Huang H, Xue HH, Gao J, Zhong XP. 2016. Critical roles of mTOR complex 1 and 2 for T follicular helper cell differentiation and germinal center responses. *eLife* **5**:e17936. DOI: https://doi.org/10.7554/eLife.17936, PMID: 27690224

Yao Y, Guo W, Chen J, Guo P, Yu G, Liu J, Wang F, Liu J, You M, Zhao T, Kang Y, Ma X, Yu S. 2018. Long noncoding RNA Malat1 is not essential for T cell development and response to LCMV infection. *RNA Biology* **15**:1477–1486. DOI: https://doi.org/10.1080/15476286.2018.1551705, PMID: 30474472

Yu D, Rao S, Tsai LM, Lee SK, He Y, Sutcliffe EL, Srivastava M, Linterman M, Zheng L, Simpson N, Ellyard JI, Parish IA, Ma CS, Li QJ, Parish CR, Mackay CR, Vinuesa CG. 2009. The transcriptional repressor Bcl-6 directs T follicular helper cell lineage commitment. *Immunity* **31**:457–468. DOI: https://doi.org/10.1016/j.immuni.2009.07.002, PMID: 19631565

Yu M, Owens DM, Ghosh S, Farber DL. 2015. Conditional PDK1 ablation promotes epidermal and T-Cell-Mediated dysfunctions leading to inflammatory skin disease. *Journal of Investigative Dermatology* **135**:2688–2696. DOI: https://doi.org/10.1038/jid.2015.232

Zeng H, Cohen S, Guy C, Shrestha S, Neale G, Brown SA, Cloer C, Kishton RJ, Gao X, Youngblood B, Do M, Li MO, Locasale JW, Rathmell JC, Chi H. 2016. mTORC1 and mTORC2 kinase signaling and glucose metabolism drive follicular helper T cell differentiation. *Immunity* **45**:540–554. DOI: https://doi.org/10.1016/j.immuni.2016.08.017, PMID: 27637146

Zhao DM, Yu S, Zhou X, Haring JS, Held W, Badovinac VP, Harty JT, Xue HH. 2010. Constitutive activation of wnt signaling favors generation of memory CD8 T cells. *The Journal of Immunology* **184**:1191–1199. DOI: https://doi.org/10.4049/jimmunol.0901199, PMID: 20026746

Zhou X, Yu S, Zhao D-M, Harty JT, Badovinac VP, Xue H-H. 2010. Differentiation and persistence of memory $CD8^+$ T cells depend on T cell factor 1. *Immunity* **33**:229–240. DOI: https://doi.org/10.1016/j.immuni.2010.08.002

Appendix 1

Appendix 1—key resources table

Reagent type (species) or resource	Designation	Source or reference	Identifiers	Additional information
Genetic reagent (*M. musculus*)	Mouse: C57BL/6J (CD45.2 and CD45.1)	Jackson Laboratory	RRID: IMSR_JAX:000664	
Genetic reagent (*M. musculus*)	Mouse: B6. Cg-Tg(Cd4-cre) 1Cwi/BfluJ (*Cd4*-Cre)	Jackson Laboratory	RRID: IMSR_JAX:022071	
Genetic reagent (*M. musculus*)	Mouse: B6. Cg-Ndor1Tg (UBC-cre/ERT2)1Ejb/2J (*Rosa26*^{CreER})	Jackson Laboratory	RRID: IMSR_JAX:008085	
Genetic reagent (*M. musculus*)	Mouse: B6. SMARTA	R. Ahmed	Emory University	
Genetic reagent (*M. musculus*)	Mouse: B6. *Pdk1*$^{fl/fl}$	W. Yuan	Chinese Academy of Medical Sciences and Peking Union Medical College	
Cell line (*H. sapiens*)	HEK293T (human embryonic kidney cells)	ATCC	Cat # CRL-3216, RRID: CVCL_0063	
Biological sample (*M. musculus*)	Primary mouse splenocytes	China Agricultural University		Freshly isolated from mice
Biological sample (*M. musculus*)	Primary mouse bone marrow cells	China Agricultural University		Freshly isolated from mice
Biological sample (*M. musculus*)	Primary mouse serum	China Agricultural University		Freshly isolated from mice
Antibody	Rat monoclonal anti-mouse CD19-PE/Cy7	Thermo Fisher Scientific	Cat # 25-0193-82, RRID: AB_657663	FACS (1:100)
Antibody	Rat monoclonal anti-mouse CD25-PE	Thermo Fisher Scientific	Cat # 12-0251-83; RRID: AB_465608	FACS (1:100)
Antibody	Rat monoclonal anti-mouse CD4-PE/Cy7	Thermo Fisher Scientific	Cat # 25-0041-82; RRID: AB_469576	FACS (1:100)
Antibody	Rat monoclonal anti-mouse CD4-APC/eFluor 780	Thermo Fisher Scientific	Cat # 47-0041-82; RRID: AB_11218896	FACS (1:100)
Antibody	Rat monoclonal anti-mouse CD4-BV510	BD Biosciences	Cat # 563106; RRID: AB_2687550	IF (1:100)
Antibody	Rat monoclonal anti-mouse/ human CD44-FITC	Thermo Fisher Scientific	Cat # 11-0441-82; RRID: AB_465045	FACS (1:100)
Antibody	Rat monoclonal anti-mouse/ human CD44-APC	Thermo Fisher Scientific	Cat # 17-0441-83; RRID: AB_469391	FACS (1:100)
Antibody	Rat monoclonal anti-mouse CD45.1-APC	Thermo Fisher Scientific	Cat # 17-0453-82; RRID: AB_469398	FACS (1:100)
Antibody	Mouse monoclonal anti-mouse CD45.1- Percp/Cy5.5	Thermo Fisher Scientific	Cat # 45-0453-82; RRID: AB_1107003	FACS (1:100)
Antibody	Mouse monoclonal anti-mouse CD45.2- APC	Thermo Fisher Scientific	Cat # 17-0454-82; RRID: AB_469400	FACS (1:100)

Continued on next page

Appendix 1—key resources table continued

Reagent type (species) or resource	Designation	Source or reference	Identifiers	Additional information
Antibody	Mouse monoclonal anti-mouse CD45.2- eFluor 506	Thermo Fisher Scientific	Cat # 69-0454-82 RRID: AB_2637105	FACS (1:100)
Antibody	Rat monoclonal anti-mouse CD62L- BV510	BioLegend	Cat # 104441; RRID: AB_2561537	FACS (1:100)
Antibody	Rat monoclonal anti-mouse CD62L- APC	Thermo Fisher Scientific	Cat # 17-0621-83; RRID: AB_469411	FACS (1:100)
Antibody	Rat monoclonal anti-mouse/ human CD45R-FITC	Thermo Fisher Scientific	Cat # 11-0452-86; RRID: AB_465056	FACS (1:100)
Antibody	Rat monoclonal anti-mouse CD45R- PerCP/Cy5.5	Thermo Fisher Scientific	Cat # 45-0451-82; RRID: AB_1107002	FACS (1:100)
Antibody	Rat monoclonal anti-mouse/ human CD45R- Biotin	Thermo Fisher Scientific	Cat # 13-0452-86; RRID: AB_466451	FACS (1:100)
Antibody	Rat monoclonal anti-mouse IgD- APC	Thermo Fisher Scientific	Cat # 17-5993-82; RRID: AB_10598660	IF (1:100)
Antibody	Rat monoclonal anti-mouse/ human GL7- eFluor 450	Thermo Fisher Scientific	Cat # 48-5902-82; RRID: AB_10870775	FACS (1:100)
Antibody	Armenian hamster monoclonal anti-mouse PD-1- PE	Thermo Fisher Scientific	Cat # 12-9985-82; RRID: AB_466295	FACS (1:100)
Antibody	Rat monoclonal anti-mouse TCR Vα2-PE	Thermo Fisher Scientific	Cat # 12-5812-82; RRID: AB_465949	FACS (1:100)
Antibody	Rat monoclonal anti-mouse/ rat Foxp3-PerCP/Cy5.5	Thermo Fisher Scientific	Cat # 45-5773-82 ; RRID: AB_914351	FACS (1:100)
Antibody	Rat monoclonal anti-mouse/ rat Foxp3-APC	Thermo Fisher Scientific	Cat # 17-5773-82 ; RRID: AB_469457	FACS (1:100)
Antibody	Rat monoclonal anti-mouse CD138-PE	BD Biosciences	Cat # 553714; RRID: AB_395000	FACS (1:100)
Antibody	Rat monoclonal anti-mouse CD138-BV421	BD Biosciences	Cat # 562610; RRID: AB_11153126	FACS (1:100)
Antibody	Armenian hamster monoclonal anti-mouse Fas-PE	BD Biosciences	Cat # 561985; RRID: AB_10895586	FACS (1:100)
Antibody	Mouse monoclonal anti-mouse/human Bcl6-PE	BD Biosciences	Cat # 561522; RRID: AB_10717126	FACS (1:40)
Antibody	Rat monoclonal anti-mouse SLAM-PE	BioLegend	Cat # 115904; RRID: AB_10895586	FACS (1:100)
Antibody	Rat monoclonal anti-mouse SLAM-APC	BioLegend	Cat # 115910; RRID: AB_493460	FACS (1:100)
Antibody	Rat monoclonal anti-mouse/ human ICOS-PE/Cy7	BioLegend	Cat # 313520; RRID: AB_10643411	FACS (1:100)
Antibody	Rat monoclonal anti-mouse IFN-γ-FITC	Thermo Fisher Scientific	Cat # 11-7311-82; RRID: AB_465412	FACS (1:100)
Antibody	Rat monoclonal anti-mouse IL-17a-PE	BD Biosciences	Cat # 559502; RRID: AB_397256	FACS (1:100)
Antibody	Rat monoclonal anti-mouse IL-4-PE/Cy7	Thermo Fisher Scientific	Cat # 25-7041-80; RRID: AB_2573519	FACS (1:100)
Antibody	Rabbit monoclonal anti-mouse/human TCF1	Cell Signaling Technology	Cat # 2203; RRID: AB_2199302	FACS (1:100)
Antibody	Rabbit monoclonal anti-mouse/rat/human PDK1	Cell Signaling Technology	Cat # 3062; RRID: AB_2236832	FACS (1:100)

Continued on next page

Appendix 1—key resources table continued

Reagent type (species) or resource	Designation	Source or reference	Identifiers	Additional information
Antibody	Rabbit monoclonal anti-mouse/human Hif1a	Cell Signaling Technology	Cat # 36169; RRID: AB_2799095	FACS (1:100)
Antibody	Rabbit monoclonal anti-mouse/rat/human FoxO1	Cell Signaling Technology	Cat # 2880; RRID: AB_2106495	FACS (1:100)
Antibody	Rabbit monoclonal anti-mouse/rat/human p-AKT^{T308}	Cell Signaling Technology	Cat # 13038; RRID: AB_2629447	FACS (1:100)
Antibody	Rabbit monoclonal anti-mouse/rat/human p-AKT^{S473}	Cell Signaling Technology	Cat # 4060; RRID: AB_2315049	FACS (1:100)
Antibody	Rabbit monoclonal anti-mouse/rat/human p-S6$^{S235/236}$	Cell Signaling Technology	Cat # 4858; RRID: AB_916156	FACS (1:100)
Antibody	Rabbit polyclone anti-mouse/rat/human p-FoxO1/3a	Cell Signaling Technology	Cat # 9464; RRID: AB_329842	FACS (1:100)
Antibody	Rabbit polyclone anti-mouse/rat/human p-PKCζ/λ	Cell Signaling Technology	Cat # 9378; RRID: AB_2168217	FACS (1:100)
Antibody	Rabbit polyclone anti-mouse/rat/human AKT	Beyotime Biotechnology	Cat # AA326	FACS (1:100)
Antibody	Rabbit monoclonal anti-mouse/human GSK3β	Beyotime Biotechnology	Cat # AF1543	FACS (1:100)
Antibody	Rabbit monoclonal anti-mouse/rat/human p-GSK3β^{S9}	Cell Signaling Technology	Cat # 5558 RRID: AB_10013750	FACS (1:100)
Antibody	Rabbit polyclone anti-mouse/rat/human p-STAT3^{S727}	Cell Signaling Technology	Cat # 9134 RRID: AB_331589	FACS (1:100)
Antibody	Rabbit monoclonal anti-mouse/rat/human STAT3	Cell Signaling Technology	Cat # 4904 RRID: AB_331269	FACS (1:100)
Antibody	Donkey polyclonal anti-rabbit IgG (minimal x-reactivity)-FITC	BioLegend	Cat # 406403; RRID: AB_893531	FACS (1:1000)
Antibody	Donkey polyclonal anti-rabbit IgG (minimal x-reactivity)-AF647	BioLegend	Cat # 406414; RRID: AB_2563202	FACS (1:1000)
Transfected construct (*M. musculus*)	MIGR1 (MSCV-IRES-GFP) (plasmid)	This paper	N/A	Retrovirus construct to transfect
Transfected construct (*M. musculus*)	MIGR1-*Tcf7* overexpressing (plasmid)	This paper	N/A	Retrovirus construct to transfect
Transfected construct (*M. musculus*)	MIGR1-*Bcl6* overexpressing (plasmid)	This paper	N/A	Retrovirus construct to transfect
Transfected construct (*M. musculus*)	MIGR1-STAT3-CA (constitutive-active) (plasmid)	This paper	N/A	Retrovirus construct to transfect
Transfected construct (*M. musculus*)	MIGR1-*Cxcr5* overexpressing (plasmid)	This paper	N/A	Retrovirus construct to transfect
Sequence-based reagent	Tcf7_F	This paper	PCR primers	CCCTTCCTGCGGATA TAGAC
Sequence-based reagent	Tcf7_R	This paper	PCR primers	GGTACACCAGA TCCCAGCAT

Continued on next page

Appendix 1—key resources table continued

Reagent type (species) or resource	Designation	Source or reference	Identifiers	Additional information
Sequence-based reagent	Cxcr5_F	This paper	PCR primers	CATGGGCTCCATCACA TACA
Sequence-based reagent	Cxcr5_R	This paper	PCR primers	GGCATGAATACCGCC TTAAA
Sequence-based reagent	Bcl6_F	This paper	PCR primers	AGACGCACAG TGACAAACCA
Sequence-based reagent	Bcl6_R	This paper	PCR primers	AGTGTGGGTCTTCAGG TTGG
Sequence-based reagent	Icos_F	This paper	PCR primers	TGCCGTGTCTTTGTC TTCTG
Sequence-based reagent	Icos_R	This paper	PCR primers	CTTCCCTTGGTCTTGG TGAG
Sequence-based reagent	Pdcd1_F	This paper	PCR primers	CTGGTCATTCAC TTGGGCTG
Sequence-based reagent	Pdcd1_R	This paper	PCR primers	AAACCA TTACAGAAGGCGGC
Sequence-based reagent	Maf_F	This paper	PCR primers	AGCAGTTGGTGACCA TGTCG
Sequence-based reagent	Maf_R	This paper	PCR primers	TGGAGATCTCCTGC TTGAGG
Sequence-based reagent	Hif1a_F	This paper	PCR primers	CCTTAACCTGTC TGCCACTTTG
Sequence-based reagent	Hif1a_R	This paper	PCR primers	TCAGCTGTGGTAA TCCACTCTC
Sequence-based reagent	Gzmb_F	This paper	PCR primers	CAAAGACCAAACGTGC TTCC
Sequence-based reagent	Gzmb_R	This paper	PCR primers	CTCAGCTC TAGGGACGATGG
Sequence-based reagent	Id2_F	This paper	PCR primers	GTCCTTGCAGGCATC TGAAT
Sequence-based reagent	Id2_R	This paper	PCR primers	TTCAACGTGTTCTCC TGGTG
Sequence-based reagent	Prdm1_F	This paper	PCR primers	ACAGAGGCCGAG TTTGAAGAGA
Sequence-based reagent	Prdm1_R	This paper	PCR primers	AAGGATGCCTCGGC TTGAA

Continued on next page

Appendix 1—key resources table continued

Reagent type (species) or resource	Designation	Source or reference	Identifiers	Additional information
Sequence-based reagent	Gata3_F	This paper	PCR primers	CTTA TCAAGCCCAAGCGAAG
Sequence-based reagent	Gata3_R	This paper	PCR primers	CATTAGCGTTCCTCC TCCAG
Sequence-based reagent	Stat3_F	This paper	PCR primers	CAATACCATTGACC TGCCGAT
Sequence-based reagent	Stat3_R	This paper	PCR primers	GAGCGACTCAAAC TGCCCT
Peptide, recombinant protein	KLH	Sigma–Aldrich	Cat# H7017	
Peptide, recombinant protein	GP_{61-80} (GLNGPDIYKGVYQFKSVEFD)	Synthesized by ChinaPeptides	N/A	
Peptide, recombinant protein	recombinant murine IL-2	R and D	Cat # 212–12	
Peptide, recombinant protein	recombinant murine IL-7	R and D	Cat # 217–17	
Commercial assay or kit	Phosflow Lyse/Fix buffer, 5X	BD Biosciences	Cat # 558049; RRID: AB_2869117	
Commercial assay or kit	Phosflow Perm buffer I	BD Biosciences	Cat # 557885 RRID: AB_2869104	
Commercial assay or kit	Caspase-3 Staining Kit	Thermo Fisher Scientific	Cat # 88-7004-42; RRID: AB_2574939	
Commercial assay or kit	Fixation/Permeabilization Solution Kit	BD Biosciences	Cat # 554714 RRID: AB_2869008	
Commercial assay or kit	Dynabeads M-280 Streptavidin	Thermo Fisher Scientific	Cat # 60210	
Commercial assay or kit	Lipofectamine 2000 Reagent	Thermo Fisher Scientific	Cat # 11668019	
Commercial assay or kit	RNeasy Mini Kit	Qiagen	Cat # 74106	
Commercial assay or kit	FastQuant RT Kit	Tiangen	Cat # KR106-02	
Commercial assay or kit	SuperReal PreMix Plus SYBR Green	Tiangen	Cat # FP205-02	
Chemical compound, drug	Freund's Adjuvant, Complete	Sigma–Aldrich	Cat # F5881	
Chemical compound, drug	Tamoxifen	Sigma–Aldrich	Cat # T5648	
Chemical compound, drug	Corn Oil	Sigma–Aldrich	Cat # C8267	

Continued on next page

Appendix 1—key resources table continued

Reagent type (species) or resource	Designation	Source or reference	Identifiers	Additional information
Chemical compound, drug	PMA	Sigma–Aldrich	Cat # P8139	
Chemical compound, drug	Ionomycin	Sigma–Aldrich	Cat # I0634	
Chemical compound, drug	Polybrene	Sigma–Aldrich	Cat # H9268	
Software, algorithm	Flowjo v10.5	Treestar	RRID: SCR_008520	
Software, algorithm	Graphpad Prism 8	Graphpad	RRID: SCR_002798	
Software, algorithm	Adobe Illustrator	Adobe	RRID: SCR_010279	
Software, algorithm	GSEA	http://www.broadinstitute.org/gsea/	RRID: SCR_003199	
Other	7-AAD	BD Biosciences	Cat # 559925 RRID: AB_2869266	
Other	PNA-FITC	Vector Laboratories	Cat # FL-1071; RRID: AB_2315097	FACS (1:500)
Other	PNA-Biotin	Vector Laboratories	Cat# BA-0074; RRID: AB_2336190	IF (1:50)
Other	Streptavidin-APC/eFluor 780	Thermo Fisher Scientific	Cat # 47-4317-82; RRID: AB_10366688	FACS (1:500)
Other	Streptavidin-eFluor 450	Thermo Fisher Scientific	Cat # 48-4317-82; RRID: AB_10359737	FACS (1:500)